Robin Guttmann, BSc

A Theoretical Study of Weak, Intermolecular Interactions in Various Systems

MASTER'S THESIS

to achieve the university degree of

Master of Science

Master's degree programme: Chemistry

submitted to

Graz University of Technology

Supervisor

Ao.Univ.-Prof. Dr.phil. Alexander F. Sax

Institute of Chemistry
University of Graz

Graz, July 2017

AFFIDAVIT

I declare that I have authored this thesis independently, that I have not used other than the declared sources/resources, and that I have explicitly indicated all material which has been quoted either literally or by content from the sources used. The text document uploaded to TUGRAZonline is identical to the present master‘s thesis.

Date

Signature

1 Publications

Parts of this master thesis are based on the following publication:

1. R. Guttmann and A. F. Sax, "Dispersion interactions and the stability of amine dimers," *ChemistryOpen*. **2017**, DOI: 10.1002/open.201700052.

Abstract

In this thesis, weak, intermolecular interactions in several systems with and without hydrogen bridges are studied. It is well known, that the interaction energy between two molecules can be decomposed in four physical meaningful components: electrostatic, exchange, induction and dispersion. Although hydrogen bonding is one of many kinds of weak, intermolecular interactions, it is often associated only with electrostatic component, whereas it is shown through this work, that all four components are important for the explanation of weak, intermolecular interaction. The interactions in various systems, main group dimers, phosphane-molecule and ethene-molecule, are calculated with symmetry-adapted perturbation theory. Many of these systems show a central atom group unit, which is often regarded as being responsible for hydrogen bonding, but neither the interaction energy nor geometry parameters of this atomic group clearly prove that it is responsible for the stabilization of such systems. To show that in such systems interaction between all atoms is responsible for the stabilization, we investigated amine dimers with alkyl substituents of various length. A density functional theory method, called dispersionless density functional plus dispersion, was used to study the size and conformational freedom of different alkyl substituted amine dimers. We show that the great variety of conformers, in alkanes and amines with big substituents, is important for the entropic part of the hydrophobic interaction in liquid alkanes.

Kurzfassung

In dieser Arbeit werden intermolekulare Wechselwirkungen in Systemen mit und ohne Wasserstoffbrückenbindungen untersucht. Die Wechselwirkungenergie zwischen zwei Molekülen besteht aus vier physikalischen Beiträgen: Elektrostatik, Austausch, Induktion und Dispersion. Entgegen der generellen Meinung, dass Elektrostatik der einzig wichtige Beitrag ist, wird gezeigt, dass alle vier Komponenten für eine sinnvolle Beschreibung miteinbezogen werden müssen. Die Wechselwirkung in verschiedenen Systemen wie Hauptgruppen-Dimere, Phosphane-Molekül- und Molekül-Ethan-Komplexe wird mit der Methode symmetrieadaptierte Störungstheorie untersucht. Viele dieser Systeme haben eine typische zentrale Wasserstoffbrücken-Einheit, jedoch ist die Argumentation für eine Stabilisierung der Systeme nur aufgrund dieser Gruppe häufig fragwürdig oder sogar falsch. Um zu zeigen, dass in solchen Systemen die Stabilisierung von allen Atomen wichtig ist, werden verschieden Alkyl-substituierte Amine untersucht. Dazu wird als Methode ein dispersionsloses Dichtefunktional mit einer Dispersionsfunktion verwendet. Anhand von verschiedener Größe und Konformation der Alkyl-Substituenten wird gezeigt, dass die Dispersion nicht zu vernachlässigen ist. Die Anzahl von nahezu energetisch äquivalenten Strukturen ist ein Maß für den entropischen Anteil der hydrophoben Wechselwirkung in flüssigen Alkanen.

2 Acknowledgments

First, I want to thank my supervisor Prof. Alexander F. Sax for his excellent support and discussions.

Many thanks to Johannes Hoja to show me the fascination of computational chemistry.

I also want to thank Prof. A. Daniel Boese for his useful programs and discussions.

Thanks to all members of the department of Physical and Theoretical Chemistry for the good atmosphere.

Furthermore I want to thank Karl Voit for his, slightly modified, LaTeX template based on KOMA script.

Finally, I want to express my deepest gratitude to my family, especially my parents, for their encouragement and their support.

Contents

3 Introduction

Weak, non covalent, interactions are often underestimated, because of their small energies, but becoming frequently more important in several fields of research and applications. Some examples can be given quite fast 1) the DNA double strand is stabilized by weak interactions (hydrogen bonding), 2) the high boiling point of alcohols compared to their alkanes is caused by hydrogen bonding, 3) solubility of compounds caused by interaction of solvent with compound, 4) stacking processes of 2D crystals is caused by adhesive forces, 5) or a recent work show the importance of non covalent interactions in synthesis.[1, 2, 3, 4, 5] Especially the role of hydrogen bonding is stressed extensively and only considered when talking about stability and properties in biological systems.[1, 2, 3, 6, 7, 8, 9]

Traditionally, hydrogen bonding is considered as the stabilization of complexes due to the occurrence of a characteristic atom group A–H$\cdots$B connecting a proton donor molecule R1–A–H to a proton acceptor molecule B–R2; R1 and R2 are substituents and A and B are atoms more electronegative than hydrogen. A–H is a polar covalent bond in the donor molecule and B is a Lewis base in the acceptor molecule. That dispersion interaction is also important for the structure of molecular complexes has been stressed only recently.[10] But also hydrophobic interactions, which are considered to be crucial for the understanding of protein folding, are dominated by dispersion interaction.[11]

Bonding means stabilization of molecular systems, it is measured by the binding

energy; if the result of bonding is called a bond, then one can say that the binding energy is a measure of the bond strength. For most chemists, bonds are also connected to atom groups having geometric properties like distances and angles, properties the central moiety A–H$\cdots$B in a hydrogen bonded complex has. In this sense, it makes sense to say that a hydrogen bond (HB) stabilizes the complex. Some chemists prefer speaking of a hydrogen bridge instead of a hydrogen bond, thus stressing structural aspects instead of aspects of stability. When we say a structure has one HB, we always claim the presence of one connecting A–H$\cdots$B group.

The concept of hydrophobic interactions was introduced by Kauzmann[12] in 1959 to explain protein folding by the analogy with the transfer of a non-polar solute from water into a non-polar solvent. According to Kauzmann the transfer is due to the poor solubility of the solute in water. Kauzmann used originally the term "hydrophobic bond", which was later replaced by "hydrophobic interaction" because there are no atom groups that can be made responsible for the bonding interaction.[13] Wolfenden and Lewis[14] explained the poor solubility of hydrocarbons in water assuming "that a strong favorable interaction among alkane molecules in liquid alkanes gives a strong favorable transfer energy for passage of an alkane from vapor into liquid alkane."[11] The term hydrophobic interactions is thus used with two different meanings, first to describe the removal of a non-polar surface from contact with water, that is a repulsive interaction; a second meaning is the direct attractive interaction between non-polar aliphatic groups, explaining, e.g., the good solubility of alkane molecules in liquid alkane mentioned by Wolfenden and Lewis.[13] Both processes involve condensed matter phases and this demands use of a free energy. Whereas the energy contribution to the free energy is caused by the basic intermolecular interactions, the explanation of the entropy contribution at the molecular level requires knowledge of the cardinality of

the set of energetically equivalent structures of interacting molecules, because the entropy of a system state is directly proportional to the logarithm of the state's degeneracy. We shall show that systems with interacting alkyl chains have a large number of equilibrium structures with similar energies and this quasi-degeneracy contributes to the entropic part of the free energy.

Weak, intermolecular interactions, also called non-covalent interactions,[15, 16] are the origin of hydrogen bonding and hydrophobic interactions with the second meaning. The stabilization energy for weakly bonded molecular systems is at least one order of magnitude smaller than that of bond energies in covalent bonds. All non-covalent interactions are caused by the four basic interactions a) electrostatics, that is the interaction between static multipoles, b) induction, that is the interaction between static multipoles in one molecule and induced multipoles in the second molecule, c) dispersion, and d) exchange repulsion, that is a repulsion between electrons due to their indistinguishability. The interaction between static multipoles may be attractive or repulsive, depending on the relative orientation of the interacting molecules. Induction can be interpreted as the classical interaction of static multipole moments in one molecule with multipoles induced in the polarizable electron density of the second molecule, it depends therefore on the static polarizabilities of the molecules involved. Induction is always attractive, it depends on the static polarizability of the molecule in which the multipole is induced. Dispersion interaction is due to the correlation of the electron motions in one molecule with those of the electrons in the other molecule and thus of purely quantum origin. The fluctuations in the electron density of one molecule, mainly caused by the non-deterministic electron motions, give rise to multipole moments, which induce multipole moments in the other molecule such that the interaction between them stabilizes the molecular system. There are however many more possible explanations of what causes the charge fluctuations or interpretations

of the dispersion interaction, see for example the book by Salam.[17] Like induction, dispersion is always attractive, its strength depends on the dynamic polarizabilities of the interacting molecules; it is a ubiquitous interaction between systems of electrons in motion and occurs also in completely non-polar systems like noble gas atoms. Nevertheless, electrostatics is frequently considered to be the most important attractive interaction in hydrogen bonded systems. Finally, exchange repulsion is a ubiquitous destabilizing interaction between indistinguishable Fermions. The amount each interaction contributes to a non-covalent interactions determines its character.

The range of the four basic interactions is very different: Exchange repulsion decreases exponentially with the distance, it has the shortest range of all basic interactions. The interaction between permanent multipoles (2^l) and (2^L), such as monopoles ($l = 0$), dipoles ($l = 1$), quadrupoles ($l = 2$) goes as $r^{-(l+L+1)}$ with the distance r between the multipoles; the range of the interaction between permanent 2^l-poles and induced 2^L-poles is much smaller than that between permanent multipoles, it goes as $r^{-2(l+L+1)}$, the same relation holds for the multipoles in dispersion interaction. For uncharged molecules, the interaction between dipoles has the longest range, this is true for permanent and for induced dipoles. Except for monopole-monopole interactions, which are indeed isotropic, all interactions between higher multipoles are genuinely anisotropic; the lowest anisotropy is found for dispersion interactions, which are therefore frequently regarded as being approximately isotropic.

Long-range or London dispersion interactions caused by the correlation of fluctuating dipoles are operative even at distances where the overlap between the wave functions of the interacting molecules is close to zero, in this case it is not necessary to antisymmetrize the product of the wave functions of the interacting molecules, when perturbation theory is used to calculate the interaction contributions. Many so

called empirical dispersion corrections schemes have been proposed for calculating long-range dispersion contributions without quantum theoretical methods. See for example reviews by Grimme. [18, 19] When the interacting molecules are so close that speaking of weakly interacting molecules becomes meaningless, electron correlation must be accounted for by proper wave functions or by using density functionals (DF) for the whole molecular system. Both types of electron correlation should merge seamlessly in the region of medium range correlation where antisymmetrization of the wave functions of the interacting molecules is mandatory and interactions between higher multipoles must be accounted for. Semilocal or hybrid Kohn-Sham DFs cannot describe long-range electronic correlation effects, and thus no London dispersion interactions, but it is not clear whether they cover a certain amount of medium or short-range dispersion interaction. It is, however, possible to develop powerful dispersion correction methods to remedy this shortcoming.[18, 19]

This work consists of three parts: In the first part, we give a discussion of general aspects about hydrogen bonded systems and theoretical insight into used methods. In part 2 we present our studies of main group complexes containing atoms of groups 14 to 17 of the periodic table. With high level methods and extrapolation schemes we study whether a hydrogen bridge is indeed responsible for the stability of these complexes. In part 3 we study the role of alkyl substituents for the stability of amine dimers. Each of these parts has a separate method section, where the different methods used for these studies are discussed.

4 Conventional view on hydrogen bonded systems

Hydrogen bonding is an attractive interaction, which was introduced to explain the stabilization of complexes containing a A–H$\cdots$B group. According to Pauling, the difference in the electronegativities of the atoms A and H is responsible for the polarity of the A–H bond in the central group, which can then interact with the acceptor atom on the same molecule (intramolecular hydrogen bonding) or another molecule (intermolecular hydrogen bonding).[2] Coulson criticised this purely electrostatic picture[20] and stated that for a reliable interpretation of hydrogen bonding all basic interactions must be taken into account.

Jeffrey used bond energies (negative interaction energy) and geometry parameters of the central group for a classification of HBs as strong, moderate and weak (see Table 4.1). An example for strong hydrogen bonded systems is F–H$\cdots$F$^-$; the dimers $(H_2O)_2$ or $(HF)_2$ are examples of systems with moderate HBs; typical systems with weak HBs are complexes of unsaturated molecules with π-systems as acceptor group and polar A–H bonds as donor group, if the the donor group is a C–H bond, some scientist speak of very weak HBs. The role of C–H bonds for the stabilization of such complexes is unclear.[2]

Table 4.1: A reduced table of Properties of strong, moderate, and weak hydrogen bonds from Jeffrey's book "An Introduction to Hydrogen Bonding".[2] Examples are given in there; our investigated dimers should be in moderate or weak class.

	Strong	Moderate	Weak
A–H$\cdots$B interaction	mostly covalent	mostly electrostatic	electrostatic
Bond lenghts	A–H$\approx$H$\cdots$B	A–H$<$H$\cdots$B	A–H$<<$H$\cdots$B
H$\cdots$B (Å)	$\sim$1.2-1.5	$\sim$1.5-2.2	$\sim$2.2-3.2
A$\cdots$B (Å)	2.2-2.5	2.5-3.2	3.2-4.0
Bond angles (°)	175-180	130-180	90-150
Bond energy (kcal mol^{-1})	15-40	4-15	$<$4
Bond energy (kJ mol^{-1})	63-167	17-63	$<$17

5 Methods

The basis of all (non relativistic) calculation in theoretical chemistry is the Schrödinger equation. In the simplest form it is given in Equation 5.1. In this formula $\hat{\mathcal{H}}$ is the Hamiltonian, which has kinetic and potential energies of nuclei and electrons, ψ is the wave function, describing a state of our system, and E is the energy.[21] Solving this eigenequation yields the energy of the system in the state considered, which is in this study always the ground state.

$$\hat{\mathcal{H}}\Psi = E\Psi \tag{5.1}$$

The first suggestion to solve this problem was introduced by Hartree, who made the assumption, that all electrons are independent from each other and each electron with a given spin (alpha or beta) is in a defined spinorbital χ. For a two electron system it is given in Equation 5.2, but can be extended easily for a many-electron system.

$$\Psi(1,2) = \chi_1(1)\chi_2(2) \tag{5.2}$$

The resulting wave function has product form with electron 1 being in one spin orbital, electron 2 in second spin orbital, etc. Beside the harsh assumption of electrons do not feel each other the major short-come is the non-asymmetry of the wave function, which should lead according to Pauli to a minus sign of the wave function when one electron is exchanged with another (indistinguishable electrons).

Therefore this ansatz must be a bit modified by taking linear combination of products of spin-orbitals (Equation 5.3).

$$\Psi(1,2) = \frac{1}{\sqrt{2}}[\chi_1(1)\chi_2(2) - \chi_1(2)\chi_2(1)] \tag{5.3}$$

The generalization of this ansatz to many electron systems is a wave function that is an antisymmetrized product of spin orbitals, called the Slater determinant. The optimized spin orbitals are the eigenfunctions of the so called Hartree-Fock operator, the iterative method for obtaining them is called the Hartree-Fock (HF) method. [21, 22] The eigenvalues corresponding to the orbitals, called the orbital energies, can be used order the orbitals. In case of an N electron system, the Slater determinant made with the N lowest orbitals, the so called occupied orbitals, is the HF ground state wave function. All other orbitals are called unoccupied or virtual orbitals.

Due to the product form of the wave function the electrons described by the spin orbitals are independent of each other and therefore uncorrelated. Each electron feels the same averaged potential stemming from all other electrons (mean-field method). The energy calculated with the exact HF orbitals is called the HF limit E_{HF}.

The correlation energy was defined by Löwdin as the difference between the exact non-relativistic energy of a system and the HF limit.[23] Technically, there are two obstacles to getting the exact non-relativistic energy E_{exact}: 1) the exact non-relativistic wave function is represented by an infinite series of Slater determinants, and 2) only approximate spin orbitals can be calculated in practice.

The methods using wave functions with more than a single Slater determinant are called post-HF methods; the improvement of the quality of the spin orbitals leads to the problem of choosing "best" basis sets.

$$E_{\text{corr}} = E_{\text{exact}} - E_{\text{HF}} \tag{5.4}$$

The wave functions used in post-HF methods are linear combinations of Slater determinants, which are obtained by replacing 1 to N occupied orbitals by unoccupied orbitals. Depending on the number of replaced occupied orbitals we speak of singly-, doubly-, triply-substituted (or excited) Slater determinants, and so on. The maximum number of orbitals that can be substituted is N. Because the HF operator has an infinite number of orbitals as eigenfunctions, substitutions of orbitals can be made in an infinite number of ways. The different post-HF methods differ in the way the occupied orbitals that are replaced by unoccupied orbitals are chosen, by the number of substitutions that are made, and by the way the unoccupied orbitals are selected.

$$\Psi_{exact} = c_0\Psi + \sum_{a}^{occ.}\sum_{r}^{virt.} c_a^r\Psi_a^r + \sum_{a,b}^{occ.}\sum_{r,s}^{virt.} c_{ab}^{rs}\Psi_{ab}^{rs} + ... \tag{5.5}$$

$c_0\Psi$ is the HF wave function, the second term $\sum_{a}^{occ.}\sum_{r}^{virt.} c_a^r\Psi_a^r$ describes all different single excitations, $\sum_{a,b}^{occ.}\sum_{r,s}^{virt.} c_{ab}^{rs}\Psi_{ab}^{rs}$ describes all different double excitations and so on. Solving this problem with all possible excitation is called Full-CI (FCI). This procedure can (even nowadays) only carried out for very small molecules, because there are a huge number of excitations and therefore high computational costs; highly depending on the number of used basis functions. Therefore we cut the exact wave function at a certain excitation (order), which leads to methods called CISD (single and double excitations) or CISDT (single, double and triple excitations). It is also possible to treat higher orders with perturbation theory, indicated with brackets, like CISD(T). A major short-come of the truncated CI methods is the size-inconsistency, which means that the energy of molecules at an infinity separated distance is not the sum of the energies of the isolated molecules. One approach

to overcome this problem in CI manner is to include some of the higher order terms; these methods are additionally named with prefix Q for quadratic, like QCISD(T).[24]

The coupled cluster (CC) method is size consistent and computationally efficient. This approach uses the cluster operator T, which acts on the reference wave function (in our case HF wave function) and produces higher excitations. The cluster operator is given by $T = T_1 + T_2 + ... + T_n$. T can be expanded as a Taylor series and rewritten in a exponential form $e^T = 1 + T + \frac{1}{2!}T^2 + ... + \frac{1}{n!}T^n$. Solving the Schrödinger equation with the wave function given by $\Psi_{\text{exact}} = e^T\Psi$ leads to energies which are a good approximation to FCI. To reduce computational costs the series are cut at a given order of excitation; leads to CC methods called CCSD, CCSD(T) etc. CCSD(T) means CC with full treatment of singles, doubles and add triplets based on perturbation theory.

Another post-HF method is Møller-Plesset-pertubation (MP) theory, which is size-consistent.[25] The unperturbed system is represented by the HF operator, the missing electron-electron interaction is treated as a perturbation. This leads to Equation 5.6. $\hat{\mathcal{H}}_0$ is the unperturbed Hamiltonian, giving the HF energy and $\lambda\hat{V}$ describes the first, second, third etc. order of perturbation, which is the extra contribution what we gain from this approach. It is clear that 1) we need to cut the series at a given order and 2) the computational costs are quite high when going to high orders. The mainly used methods cut the series at second, third or fourth term, called then MP2, MP3 and MP4.

$$(\hat{\mathcal{H}}_0 + \lambda\hat{V})\Psi = (E_0 + E_1 + ...)\Psi \tag{5.6}$$

Another approach is the density functional theory (DFT). These methods work with densities. Equation 5.7 shows the general DFT expression (depending on the density) for the energy $E_{\text{DFT}}[\rho]$, where $T[\rho]$ is the kinetic energy calculated

from one-electron density, $E_{\mathrm{ne}}[\rho]$ is the attraction between nucleus and electron, $J[\rho]$ is the coloumb energy, and $E_{\mathrm{xc}}[\rho]$ is the exchange-correlation energy. $T[\rho]$, $E_{\mathrm{ne}}[\rho]$ and $J[\rho]$ are well known and can be calculated quite easily, whereas the $E\mathrm{xc}[\rho]$ term is unknown and includes parts of the potential and remaining kinetic energy. Therefore approximations have to be used, which then lead to different functionals.[21] Most of them have the problem that they are not describing the long-range dispersion interaction correctly, but as already mentioned empirical dispersion correction can be used to cure this deficiency.

$$E_{\mathrm{DFT}}[\rho] = T[\rho] + E_{\mathrm{ne}}[\rho] + J[\rho] + E_{\mathrm{xc}}[\rho] \tag{5.7}$$

With these methods, the interaction energy can be calculated in the supermolecule approach as difference of the energy of the interacting complex AB and the sum of the energies of the isolated molecules A and B. The interaction energy E_{Int} is defined as the energy of the system subtracting the energies of the subsystems (see Equation 5.8). If $E_{\mathrm{Int}} < 0$, the complex is stabilized, otherwise it is destabilized.

$$E_{\mathrm{Int}} = E(\mathrm{AB}) - (\mathrm{E(A)} + \mathrm{E(B)}) \tag{5.8}$$

The supermolecule approach has major shortcomes: 1) three energy calculations are needed, 2) the choice of the correct basis set, 3) the contributions of the four basic interactions are not known. If we want to know the magnitude of the contributions, we need another approach, namely symmetry-adapted perturbation theory (SAPT).[26]

For the discussion of SAPT we follow the book by Stone.[16] The interaction energy is the mutual perturbation of the interacting molecules, the non-interacting molecules represent the unperturbed system. The Hamiltonian for the interacting system is the sum of the Hamiltonian for the unperturbed system and the perturbation V. The Hamiltonian for the unperturbed system is the sum of the

two Hamiltonian for the molecules. Therefore the wave function of the interacting system has product form. By using the antisymmetry operator the antisymmetry character of the final wave function is achieved (the single wave functions of A and B are already antisymmetric). The underlying wave function determines, what need to be included by the perturbation. If the monomers are described by uncorrelated wave functions, the perturbation must account for both intra- and intermolecular correlation. When DFT is used to describe the monomers, the intra-molecular correlation is already represented by the Kohn-Sham orbitals and perturbation theory is needed for the calculation of the inter-molecular interaction only; the method is called SAPT(DFT). The wrong asymptotic behavior of the exchange-correlation potential at long distances is a problem for the calculation of long-range contributions in SAPT(DFT). One must correct the exchange-correlation potential in such a way that it fits well in short, medium and long distances, when applying the correction. Several asymptotic corrections are used like those from Tozer-Handy or Grüning, which differs in switching (activation of the correction) functions and used potentials (see also Appendix).[27, 28]

With all these variants of SAPT the final interaction energy is given by Equation 5.9. It is decomposed in the four above explained components: electrostatic E_{elst}, exchange E_{exch}, induction E_{Ind} and dispersion E_{D}.

$$E_{\text{Int}} = E_{\text{elst}} + E_{\text{exch}} + E_{\text{Ind}} + E_{\text{D}} \tag{5.9}$$

In following, we will use the term interaction energy for all interaction components especially for their representations by graphs; stabilization energy means always the difference between the energies of the dissociated dimer and it equilibrium geometry; we abstain from using the term hydrogen bond energy. When we say in this work that an interaction energy is smaller than another, we speak about the absolute values.

System stabilization is a process related to changes of the system geometry. To get the distance dependence of the interaction energy without intramolecular energy contributions from relaxation of the interacting molecules, especially in the second part we study the energy curves for rigid dissociation of the dimer. For doing this, we optimized the equilibrium geometries of the dimers and then separated the monomers without allowing geometry relaxation.

6 Basis set problem

Molecular orbitals (MOs) are linear combinations of atomic orbitals (AOs). To describe the AOs we use a sum of Gaussian functions, which is the basis set (BS); one function for each orbital would correspond to minimal basis set, others are called extended and lead in general to better description of the molecule and therefore lower energies.

In this work we use Dunning's unaugmented basis sets cc-pVXZ and the augmented basis sets aug-cc-pVXZ (X=D,T,Q and 5);[29, 30, 31, 32] as shorthand notation we use in following XZ (X=D,T,Q and 5) for the unaugmented and aXZ for the corresponding augmented basis sets.

In general all basis sets are finite and this incomplete describtion leads to two errors: the basis set incompleteness error (BSIE) and the basis set superposition error (BSSE).

The BSIE arises from the not fully converged energy, when using a finite basis set. Even if we increase the size of the basis set we make a noticeable error, because the complete basis set (CBS) contains an infinite number of basis functions. The energy value for a complete basis set is the CBS limit. Several recipes are proposed in the literature to get a approximation for the CBS value; for example the F12 method or extrapolation schemes.[33, 21]

In this work we use the extrapolation scheme (see Equation 6.1) proposed by Helgaker et al.[34] and modified by Schwenke.[35] The difference is the different

exponent in the denominator of the $(\frac{Y}{Y-1})$ term; labelled l^{-5} and l^{-3}, l being the angular moment quantum number of the largest polarisation function of the used BS. l^{-5} is used for HF part,[36, 37] and for correlation part l^{-3}, since it is slower converging.[34] The BS from Dunning is used, which are designed for a systematic (exponential) convergence and therefore first choice for extrapolation.

$$E_{\mathrm{CBS}} = E_{\mathrm{cc-pVYZ}} + \frac{E_{\mathrm{cc-pVYZ}} - E_{\mathrm{cc-pV(Y-1)Z}}}{(\frac{Y}{Y-1})^{\mathrm{exp=3or5}} - 1} \tag{6.1}$$

For Equation 6.1 typically two calculations with neighbouring angular moment are needed (e.g. aDZ and aTZ or aTZ and aQZ). In following the short hand notion of [small basis set/high basis set] is used like [aDZ/aTZ]; showing a extrapolation with aug-cc-pVDZ and aug-cc-pVTZ to the estimated CBS.

For several methods like CCSD(T), HF, SAPT(DFT) and certain DF the basis set convergence is different, but well known. For the dlDF functional the basis set convergence is not well established and the reason for an extensive study of the basis set convergence. It is important to mention, that for SAPT calculations the basis set used must contain diffuse functions to describe the mid-bond space and give accurate numbers.

The second error, BSSE, is important for the calculation of interaction energies using the supermolecule approach. Isolated molecule A is described by basis set BSA; isolated molecule B is described by basis set BSB, but the interacting complex is described by the sum of basis sets BSA and BSB. Acoordingly, the energies of the three systems are calculated with three different basis sets which makes them uncomparable. The widely used remedy is the counter-poise (CP) correction by Boys and Bernadi,[38] where for both isolated molecules the same basis is used as for the complex. The formula for the interaction energy is given in Equation 6.2;

CP indicates the counterpoise corrected values.

$$E_{\mathrm{Int,CP}} = E(AB) - (E(A)_{\mathrm{CP}} + E(B)_{\mathrm{CP}}) \tag{6.2}$$

Important aspects to consider:

1. CP corrected interaction energy leads to a less stabilized system; the energy of the dimer is the same, but both monomers have a lowering in energy.
2. With increasing basis set the BSSE is becoming less important; the reason is the better description at the monomer level and the additional functions from other monomer does not affect that much
3. Methods which never calculate the supermolecule have no BSSE; one example is SAPT

A work from Burns et al. discuss such high level methods with or without counterpoise correction in combination with extrapolation quite extensively.[39]

All these points leads to the conclusion that optimum way to do these calculations is to use extrapolation methods for dimer and monomers (minor error by BSEI) and then use these energies with CP corrected supermolecule approach (to reduce BSSE). Other important requirements are the size consistency and that the full correlation energy has to be included; for instance in HF and plane DFT certain amount is missing. To avoid all these kind of errors we mainly use the wave function method CCSD(T), the perturbation based method SAPT(DFT) and a special designed DFT method with dispersion correction.

7 Interaction of homo- and hetero-molecular complexes

7.1 Programs and used basis sets

The SAPT(DFT) calculations were mainly performed with the MolPro2010 suite of programs by using the density fitting approach.[40, 41] The PBE0AC functional was used as recommended by the authors of the method;[42] together with the basis sets aTZ and aQZ. For the monomer calculations we used the asymptotic correction of Gruening;[28] the used ionization potentials, defined as the difference of the cation and the neutral system, and energies of the highest occupied molecule orbitals were calculated for every molecule with the same, uncorrected functional with the basis set a5Z. The reference CCSD(T) calculation were calculated with the TURBOMOLE suite of programs.[43] To speed up the calculations the resolution of identity approximation for the post-HF methods were used. [44, 45]

For the common main group dimers starting structures were obtained from BEGDB and all others were drawn or arranged within Avogadro.[46, 47] In TURBOMOLE all geometries were preoptimized with the method B3LYP combined with Grimme‘s approach D3 and the basis set super position error by using the counterpoise correction by Boys and Bernadi.[48, 49] The basis set was aTZ.

To obtain the minimum configurations we used the high level method QCISD(T)

as implemented in MolPro2010. For the gradients extrapolation we use the program QMPOT.[50] The following extrapolation scheme was applied:

$$E/G_{\mathrm{QCISD(T)}} = E/G_{\mathrm{HF}}[aTZ/aQZ] + \Delta E/G_{\mathrm{MP2}}[aTZ/aQZ] + \Delta E/G_{\mathrm{QCISD(T)}}[aDZ] \tag{7.1}$$

These procedure leads to structures, which are very close to CCSD(T) ones. [51, 52]

The slowest converging SAPT(DFT) components is the dispersion component; if not other mentioned the dispersion part of the SAPT(DFT) energy calculations was extrapolated with the forumla l^{-3} with [aTZ/aQZ], like it is done in a similar way in the paper of Rezac and co-workers.[53] As suggested in a recent work about basis set limit coupled cluster by Boese we used for the CP corrected CCSD(T) calculations within the TURBOMOLE suite of programs different scheme depending on convergence and computional cost of the different parts;[52] for Hartree-Fock (HF), the missing correlation energy added by Møller-Plesset-Perturbation-Theory second order $\Delta \mathrm{E}_{\mathrm{MP2}}$ and coupled cluster $\Delta \mathrm{E}_{\mathrm{CCSD(T)}}$:

$$E_{\mathrm{CCSD(T)}} = E_{\mathrm{HF}}[a5Z/a6Z] + \Delta E_{\mathrm{MP2}}[a5Z/a6Z] + \Delta E_{\mathrm{CCSD(T)}}[aTZ/aQZ] \tag{7.2}$$

An extensive discussion of the basis set convergence and optimal extrapolation schemes are given in the paper of Boese.[52]

7.1.1 Comparison of SAPT(DFT) with CCSD(T)

Several papers discuss how to obtain very good SAPT(DFT)/CBS in comparison to CCSD(T)/CBS values. [53] Table 7.1 lists the absolute and relative (in percentage) errors of all structures discussed in this work. There is a different behavior of first and second period; the mean relative error at the first period is below 14 % and at the second period it is up to nearly 40 %. The largest errors have the complexes with (H_2S) and (HCl). Excluding these two molecules from the set, the error of all molecules is below 23 %. As already mentioned in the method section the problem

in using DFT for monomer calculations is the wrong behavior of the asymptotic behavior of the exchange-correlation potential, which is cured in MolPro2010 by the asymptotic correction by Grüning.[28].

The genuine SAPT code by Szalewicz and coworkers was used to calculate SAPT(DFT) interaction energies with density fitting approach;[54, 55, 56, 57] using DALTON and GAMESS for the monomer calculations.[58, 59] This code uses the asymptotic correction from Tozer and Handy.[27] In contrast to the correction in MolPro2010 it uses only the ionization potential and recommended to use experimental obtained ones.

Using the Deleware version with ionization potentials taken from literature,[60] the same basis sets aTZ and functional PBE0AC to calculate the SAPT(DFT)/CBS values for $(H_2S)_2$ and $(HCl)_2$, we obtain interaction energies which are more close to the CCSD(T)/CBS values ($(H_2S)_2$ -18.3 % and $(HCl)_2$ -8.2 %). The deviation in the total interaction energies between both implementations must be also present in the single components. The biggest deviation was found for the exchange component with around 3-4 kJ/mol.

The question is now arising: why are these two version different? The differences may be due to 1) different implementation of SAPT(DFT), 2) different asymptotic corrections, 3) that experimental ionization potentials are used in the Delaware code, whereas in MolPro2010 these are calculated.

According to these findings we can say that the results for the first period are quite good; for the second period they can be problematic.

Table 7.1: Absolute in kJ/mol and relative error in % (brackets) of SAPT(DFT) results according to the reference CCSD(T) values; Mol means Molecule.

	CH_4	NH_3 C_s	H_2O	HF
Dimer	0.12 (5.6)	0.70 (5.4)	-0.08 (-0.4)	-0.75 (-3.9)
Mol-PH_3	0.06 (2.0)	-0.08 (-1.5)	-0.96 (-9.0)	-2.16 (-10.3)
PH_3-Mol		-0.05 (-1.0)	-0.32 (-7.7)	-0.35 (-14.3)
Mol-Ethan	-0.23 (-11.6)	0.09 (1.4)	-1.11 (-10.6)	-2.77 (-14.8)
	SiH_4	PH_3	H_2S	HCl
Dimer	-0.03 (-1.0)	-0.36 (-6.5)	-2.27 (-33.0)	-2.61 (-32.6)
Mol-PH_3	0.14 (3.6)		-2.21 (-39.0)	-4.03 (-30.0)
PH_3-Mol			-0.76 (-29.5)	0.30 (9.4)
Mol-Ethan	-0.26 (-22.5)	-0.45 (-17.1)	0.16 (2.6)	-3.99 (-32.3)

7.2 Results

Three groups of complexes will be presented and discussed: dimers containing electronegative main group elements of groups 14 to 17, (PH_3)-(molecule) complexes, and (molecule)-ethene complexes. (PH_3)-(molecule) means that PH_3 is the donor molecule and (molecule) is the acceptor. In (molecule)-ethene complexes is (molecule) the donor and ethene is the acceptor molecule. The first group of dimers allows to study how the four basic interactions determine structure and stability of the complexes in moderate to weak HBs. The second group covers complexes with a donor molecule that looks like a typical donor molecule but has extremely small bond dipoles. In the third group, the donor molecules having no molecular dipole moment and extremely weak bond dipoles, and the acceptor is not an atom with lone pairs but a molecule with a easily polarizable π bond.

7.2.1 Dimers

The equilibrium geometries of the investigated main group dimers are shown in Figure 7.1. Not all structures contain the typical central unit of a hydrogen bonded system. The geometry parameters in Table 7.2 and the interaction energies in Table 7.3 show, that these systems are mainly stabilized by dispersion interaction.

Table 7.2: Geometry parameters of the central group of the investigated dimers, X is the non hydrogen atom; distances in Å and angles in °.

Dimer	X···X	X–H	H···X	X–H···X
$(CH_4)_2$	3.66			
$(NH_3)_2$ C_s	3.25	1.02	2.28	161
$(NH_3)_2$ C_{2h}	3.17	1.01	2.52	122
$(H_2O)_2$	2.91	0.96	1.96	171
$(HF)_2$	2.73	0.92	1.81	170
$(SiH_4)_2$	4.31			
$(PH_3)_2$	3.68			
$(H_2S)_2$	4.16	1.34	2.82	174
$(HCl)_2$	3.78	1.28	2.52	167

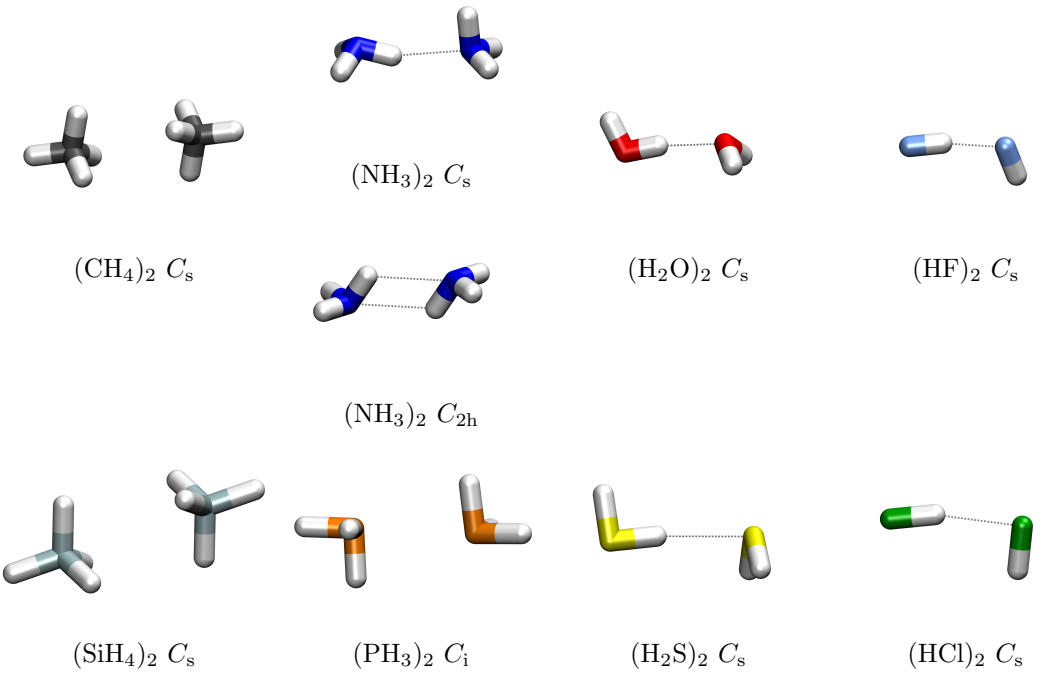

Figure 7.1: Different structures of the investigated molecules including their symmetry.

Table 7.3: SAPT and CCSD(T) results of the different main group dimers; distances are in Å and energies are in kJ mol^{-1}.

Dimer	R(X-X)	E_{elst}	E_{exch}	E_{Ind}	E_{D}	E_{SAPT}	$E_{\text{CCSD(T)}}$
$(CH_4)_2$	3.66	-0.80	3.22	-0.15	-4.30	-2.03	-2.16
$(NH_3)_2$ C_s	3.25	-21.36	22.51	-5.25	-8.23	-12.32	-13.02
$(NH_3)_2$ C_{2h}	3.17	-19.84	19.14	-3.25	-8.24	-12.19	-13.05
$(H_2O)_2$	2.91	-32.83	30.14	-8.95	-9.29	-20.93	-20.85
$(HF)_2$	2.73	-27.02	23.61	-9.15	-7.26	-19.82	-19.08
$(SiH_4)_2$	4.30	-0.11	2.27	-0.21	-4.64	-2.70	-2.67
$(PH_3)_2$	3.68	-6.27	11.37	-1.92	-9.04	-5.86	-5.50
$(H_2S)_2$	4.16	-8.69	9.67	-3.34	-6.81	-9.16	-6.89
$(HCl)_2$	3.78	-9.68	11.72	-5.17	-7.48	-10.61	-8.00

7.2.1.1 Group 17

The HF dimer has the structure of a typical hydrogen bonded system: the donor F–H bond points to the F atom in the acceptor molecule; the F$\cdots$F distance is 2.73 Å and the F–H$\cdots$F angle is 170 °. The stabilization energy is -19.82 kJ/mol; the contributions of the four basic interactions are -27.02 kJ/mol (E_{elst}), 23.61 kJ/mol (E_{exch}), -9.15 kJ/mol (E_{Ind}) and -7.26 kJ/mol (E_{D}). The absolute values of the electrostatic and exchange interactions are larger than the absolute value of the total interaction energy. According to stabilization energy and geometry parameters, the HF dimer is a moderate hydrogen bonded system.

The HCl dimer has the structure of a typical hydrogen bonded system: the donor Cl–H bond points to the Cl atom in the acceptor molecule; the Cl$\cdots$Cl distance is 3.78 Å and the Cl–H$\cdots$Cl angle is 167 °. The stabilization energy is -10.61 kJ/mol; the contributions of the four basic interactions are -9.68 kJ/mol (E_{elst}), 11.72 kJ/mol

(E_{exch}), -5.17 kJ/mol (E_{Ind}) and -7.48 kJ/mol (E_{D}). The classification of the HCl dimer is not unambiguous, according to the stabilization energy it is a weak HB system but a moderate HB system according to the Cl–H$\cdots$Cl angle.

Comparison of the two dimers of group 17 shows similar A–H$\cdots$B angles; that the distance between the atoms A and B are different in the two complexes is not surprising. The stabilization energy of $(HCl)_2$ is roughly half of the stabilization energy of $(HF)_2$; the same is true for all components but the dispersion interaction, which is roughly the same in both complexes. Accordingly, $(HCl)_2$ is by 0.2 kJ/mol more stabilized than $(HF)_2$. The reduction of the interaction energies is in accord with the much larger Cl$\cdots$Cl distance; that the Cl atoms have a much larger polarizability than the F atoms explains why the dispersion contribution is even larger than in the HF dimer.

7.2.1.2 Group 16

The H_2O dimer is the prototype of a system with a moderate HB: one O–H bond in the donor molecule points to the O atom in the acceptor molecule, the O$\cdots$O distance is 2.91 Å and the O–H$\cdots$O angle is 171 °. The stabilization energy is -20.93 kJ/mol; the contributions of the four basic interactions are -32.83 kJ/mol (E_{elst}), 30.14 kJ/mol (E_{exch}), -8.95 kJ/mol (E_{Ind}) and -9.29 kJ/mol (E_{D}). Stabilization energy and bond angle are typical for a moderate HB.

The structure of the H_2S dimer is quite similar to that of the H_2O dimer: one S–H bond in the donor molecule points to S atom in the acceptor molecule, the S$\cdots$S distance is 4.16 Å and the S–H$\cdots$S angle is 174 °. The stabilization energy is -9.16 kJ/mol; the contributions of the four basic interactions are -8.69 kJ/mol (E_{elst}), 9.67 kJ/mol (E_{exch}), -3.34 kJ/mol (E_{Ind}) and -6.81 kJ/mol (E_{D}). According to the stabilization energy, the H_2S dimer has a weak HB, but a moderate HB according to the S–H$\cdots$S angle.

The A–H$\cdots$B angles in $(H_2O)_2$ and $(H_2S)_2$ are quite similar; the S$\cdots$S distance is by 1.2 Å larger than the O$\cdots$O distance, and the stabilization energy of $(H_2S)_2$ is reduced by a factor of 2; the interaction contributions are lowered by factors of 2 to 3, only E_D is reduced by only 30 %. Again, the increase of the polarizability of the S atom outweighs the reduction of dispersion interaction due to the larger S$\cdots$S distance.

7.2.1.3 Group 15

According to its structure, the NH_3 dimer is a typical hydrogen bonded system. Two structures of the ammonia dimer were obtained; one with C_s symmetry and a single HB; and one with C_{2h} and two HBs. The N$\cdots$N distance in the C_s structure is 3.25 Å and the N–H$\cdots$N angle is 161 °. In the C_{2h} structure, the N$\cdots$N distance is 3.17 Å and the N–H$\cdots$N angle is 120 °. The largest difference between both structures is found for the N–H$\cdots$N angle. The stabilization energies and the basic contributions for both structures are quite similar; for the C_s structure it is -12.32 kJ/mol and the basic contributions are -21.36 kJ/mol (E_{elst}), 22.51 kJ/mol (E_{exch}), -5.25 kJ/mol (E_{Ind}) and -8.23 kJ/mol (E_D). The C_{2h} structure is slightly less stable and has a stabilization energy of -12.19 kJ/mol and the basic contributions are -19.84 kJ/mol (E_{elst}), 19.14 kJ/mol (E_{exch}), 3.25 kJ/mol (E_{Ind}) and -8.24 kJ/mol (E_D). According to the geometry parameters and the stabilization energy is the NH_3 dimer a weakly bonded HB system.

The PH_3 dimer is a stable complex without a bridging hydrogen atom. The symmetry of the dimer is C_i; the P$\cdots$P distance is 3.68 Å; all P–H bonds have the same length and all H–P–H angles are nearly 90 ° (see Figure 7.1). The stabilization energy is -5.86 kJ/mol and the basic contributions are -6.27 kJ/mol (E_{elst}), 11.37 kJ/mol (E_{exch}), -1.92 kJ/mol (E_{Ind}) and -9.04 kJ/mol (E_D).

To find out whether there is any kind of stabilization in a complex with a hydrogen

Table 7.4: Interaction energies in kJ/mol of phosphane dimer at different rotation angles alpha in ° and a P···P distance of 3.7 Å; the basis set aTZ was used.

α	E_{elst}	E_{exch}	E_{Ind}	E_{D}	E_{SAPT}
0	-5.98	10.71	-1.78	-8.14	-5.18
75	-18.91	59.22	-12.80	-18.48	9.03
180	-16.99	53.36	-10.99	-17.55	7.83

bridge, the potential energy surface for the rigid rotation of one phosphane molecule in $(PH_3)_2$ was calculated (see later Figure 7.5).

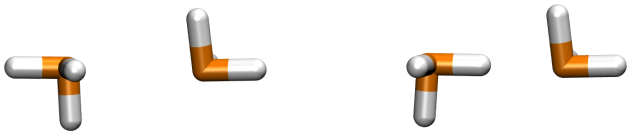

Figure 7.2: Different PH_3 dimer structures; equilibrium structure with no hydrogen bridge (left) and non equilibrium structure with a hydrogen bridge (right)

The rotation was performed for different P···P distances. The rotation axis goes through the P atom of the rotating molecule and is orthogonal to the line going through the two P atoms, it is nearly coincident with a P–H bond. The equilibrium structure without a linear hydrogen bridge correspond to a rotation angle of zero degree. The interaction is repulsive for all structures with nearly linear hydrogen bridges. The origin is the strong repulsion, which outweighs the extra stabilization coming from electrostatic, induction and dispersion contribution; shown in Table 7.4.

Constrained optimization of $(PH_3)_2$ with a linear hydrogen bridge (see Figure 7.2) yields a P···P distance of 4.50 Å, a stabilization energy of -2.27 kJ/mol with components of -1.62 kJ/mol (E_{elst}), 4.93 kJ/mol (E_{exch}), -0.89 kJ/mol (E_{Ind}) and

-4.70 kJ/mol (E_{D}). Compared to the phosphane dimer with no hydrogen bridge the distance is by roughly 0.8 Å longer and all contributions are halved.

The dimers in this group are quite different and hard to compare, because $(PH_3)_2$ has no clear hydrogen bond. When going from $(NH_3)_2$ to $(PH_3)_2$ the stabilization energy and all components are decreasing except the E_{D} contribution, which is by the small amount of 0.8 kJ/mol more stabilizing.

7.2.1.4 Group 14

The CH_4 dimer is a system without a typical central group. The monomers have nearly undisturbed T_{d} symmetry. The distance C$\cdots$C is 3.66 Å. The stabilization energy is very small with -2.03 kJ/mol and the basic contributions are -0.80 kJ/mol (E_{elst}), 3.22 kJ/mol (E_{exch}), -0.15 kJ/mol (E_{Ind}) and -4.30 kJ/mol (E_{D}). Electrostatics and induction contribute together less than -1.0 kJ/mol, the exchange is roughly three times as large (absolute values), but the stabilization is solely due to the large dispersion contribution.

Also the SiH_4 dimer does not have a central group; the monomers have again T_{d} symmetry. The Si$\cdots$Si distance is 4.30 Å. The stabilization energy is -2.70 kJ/mol and the basic contributions are -0.11 kJ/mol (E_{elst}), 2.27 kJ/mol (E_{exch}), -0.21 kJ/mol (E_{Ind}) and -4.64 kJ/mol (E_{D}).

The $(SiH_4)_2$ dimer is slightly more stable than $(CH_4)_2$ although electrostatic and induction contribution are smaller than for the methane dimer. The reason for the higher stabilization is a lower repulsive exchange and a higher attractive dispersion interaction.

7.2.2 Phospane-(molecule) and (molecule)-phosphane

Stable $(PH_3)_2$ has no hydrogen bridge. To find out whether the acceptor atom B is responsible for this, we studied (PH_3)-(molecule) complexes where (molecule)

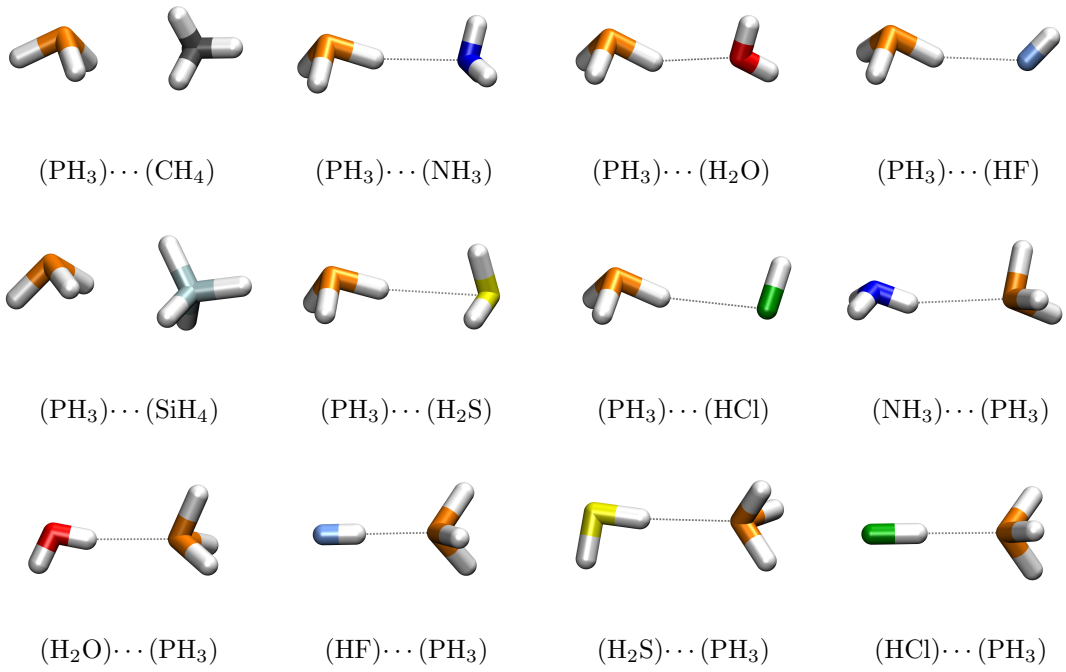

Figure 7.3: Different structures of the investigated phosphane-molecule and molecule-phosphane complexes.

represents all other main group monomers. These complexes have the central group P–H$\cdots$B. On the other hand, also the electronegativity of the acceptor atom B is thought to be decisive for the stability of a hydrogen bonded complexes. Since phosphorous has a low electronegativity , we varied the nature of the donor group A–H in the complexes (molecule)-(PH_3) with the central group A–H$\cdots$P. The equilibrium structures of these mixed complexes are given in Figure 7.3; geometries and stabilization energies depend on whether PH_3 is donor or acceptor molecule (see Figure 7.3 and Table 7.5). For the (PH_3)-(CH_4) and (PH_3)-(SiH_4) no hydrogen bridged structure was found. All energies are given in Table 7.6.

Table 7.5: Geometry parameters of the central group of the investigated (PH_3)-molecule and molecule-(PH_3) complexes, X is the non hydrogen atom; distances in Å and angles in °.

Donor	P···X	P–H	H···X	P–H···X
(CH_4)	3.77			
(NH_3)	4.09	1.42	2.71	164
(H_2O)	3.88	1.42	2.58	151
(HF)	3.98	1.42	2.69	150
(SiH_4)	4.16			
(H_2S)	4.56	1.42	3.18	164
(HCl)	4.44	1.41	3.13	153
Acceptor	X···P	X–H	H···P	X-H···P
(NH_3)	3.95	1.01	3.00	157
(H_2O)	3.58	0.96	2.63	169
(HF)	3.28	0.93	2.35	180
(H_2S)	4.27	1.34	2.93	174
(HCl)	3.84	1.29	2.55	179

Table 7.6: SAPT and CCSD(T) results of the different main group phosphane-molcules and molecule-phosphane complexes; distances are in Å and energies are in kJ mol^{-1}.

Acceptor	R(P-X)	E_{elst}	E_{exch}	E_{Ind}	E_{D}	E_{SAPT}	$E_{\text{CCSD(T)}}$
(CH_4)	3.77	-1.86	5.05	-0.44	-5.94	-3.18	-3.25
(NH_3)	4.09	-6.34	9.37	-2.4	-5.23	-4.60	-4.55
(H_2O)	3.88	-4.60	5.94	-1.45	-4.32	-4.43	-4.11
(HF)	3.98	-2.22	2.37	-0.54	-2.44	-2.83	-2.47
(SiH_4)	4.16	-1.92	6.1	-0.66	-7.15	-3.63	-3.76
(H_2S)	4.56	-2.49	4.82	-0.90	-4.76	-3.33	-2.57
(HCl)	4.44	-1.84	2.91	-0.48	-3.51	-2.91	-3.22
Donor	R(X-P)	E_{elst}	E_{exch}	E_{Ind}	E_{D}	E_{SAPT}	$E_{\text{CCSD(T)}}$
(NH_3)	3.95	-6.06	6.91	-1.55	-4.70	-5.40	-5.32
(H_2O)	3.58	-14.94	16.62	-5.77	-7.45	-11.54	-10.58
(HF)	3.28	-28.29	31.02	-16.04	-9.84	-23.14	-20.98
(H_2S)	4.27	-7.67	9.28	-3.16	-6.33	-7.89	-5.67
(HCl)	3.84	-19.28	23.93	-11.63	-10.46	-17.45	-13.42

7.2.2.1 Group 17

7.2.2.1.1 (PH_3)-(HF) and (PH_3)-(HCl)

(PH_3)-(HF) contains a P–H bond pointing to the F atom. The P$\cdots$F distance is 3.98 Å and the angle is 150 °. The stabilization energy is -2.83 kJ/mol, and the basic contributions are -2.22 kJ/mol (E_{elst}), 2.37 kJ/mol (E_{exch}), -0.54 kJ/mol (E_{Ind}) and -2.44 kJ/mol (E_{D}).

(PH_3)-(HCl) contains a P–H bond pointing to the Cl atom. The P$\cdots$Cl distance is 4.44 Å and the angle is 153 °. The stabilization energy is -2.91 kJ/mol, and the basic contributions are -1.84 kJ/mol (E_{elst}), 2.91 kJ/mol (E_{exch}), -0.48 kJ/mol (E_{Ind}) and -3.51 kJ/mol (E_{D}).

The angles of the central groups are nearly identical. The stability of both complexes is very similar with (PH_3)-(HCl) being slightly more stable than (PH_3)-(HF), although electrostatics is larger and exchange is smaller in (PH_3)-(HF) than in (PH_3)-(HCl). This is outweighed by the 1.1 kJ/mol larger dispersion contribution, probably due to the larger polarizability of the chlorine atom, resulting in the higher stabilization of (PH_3)-(HCl).

7.2.2.1.2 (HF)-(PH_3) and (HCl)-(PH_3)

(HF)-(PH_3) contains a F–H bond pointing to the P atom. The F$\cdots$P distance is 3.28 Å and the angle is 180 °. This is a example of a HB with a linear central group. The stabilization energy is -23.14 kJ/mol and the basic contributions are -28.29 kJ/mol (E_{elst}), 31.02 kJ/mol (E_{exch}), -16.04 kJ/mol (E_{Ind}) and -9.84 kJ/mol (E_{D}).

(HCl)-(PH_3) contains a Cl–H bond pointing to the P atom. The Cl$\cdots$P distance is 3.84 Å and the angle is 179 °. The stabilization energy is -17.45 kJ/mol and the basic contributions are -19.28 kJ/mol (E_{elst}), 23.93 kJ/mol (E_{exch}), -11.63 kJ/mol (E_{Ind}) and -10.46 kJ/mol (E_{D}).

Both complexes have linear central groups. The stabilization energies are by a factor of 10 larger than in the complexes with PH_3 as donor molecule, according to them the complexes have moderate HBs. In both complexes, exchange outweighs electrostatics and induction is larger than the dispersion contribution.

7.2.2.2 Group 16

7.2.2.2.1 (PH_3)-(H_2O) and (PH_3)-(H_2S)

(PH_3)-(H_2O) contains a P–H bond pointing to the O atom. The P$\cdots$O distance is 3.88 Å and the P–H$\cdots$O angle is 151 °. The stabilization energy is -4.43 kJ/mol and the basic contributions are -4.60 kJ/mol (E_{elst}), 5.94 kJ/mol (E_{exch}), -1.45 kJ/mol (E_{Ind}) and -4.32 kJ/mol (E_{D}).

(PH_3)-(H_2S) contains a P–H bond pointing to the S atom. The P$\cdots$O distance is 4.56 Å and the P–H$\cdots$O angle is 164 °. The stabilization energy is -3.33 kJ/mol and the basic contributions are -2.49 kJ/mol (E_{elst}), 4.82 kJ/mol (E_{exch}), -0.90 kJ/mol (E_{Ind}) and -4.76 kJ/mol (E_{D}).

According to the stabilization energies, both complexes have weak HBs with (PH_3)-(H_2O) being more stable than (PH_3)-(H_2S). All contributions in (PH_3)-(H_2O) are larger than in (PH_3)-(H_2S), only the dispersion contribution is in (PH_3)-(H_2S) larger.

7.2.2.2.2 (H_2O)-(PH_3) and (H_2S)-(PH_3)

(H_2O)-(PH_3) contains a O–H bond pointing to the P atom. The O$\cdots$P distance is 3.57 Å and the O–H$\cdots$P angle is 169 °. The stabilization energy is -11.54 kJ/mol and the basic contributions are -14.94 kJ/mol (E_{elst}), 16.62 kJ/mol (E_{exch}), -5.77 kJ/mol (E_{Ind}) and -7.54 kJ/mol (E_{D}).

(H_2S)-(PH_3) contains a S–H bond pointing to the P atom. The S$\cdots$P distance is 4.27 Å and the O–H$\cdots$P angle is 174 °. The stabilization energy is -7.89 kJ/mol and

the basic contributions are -7.67 kJ/mol (E_{elst}), 9.28 kJ/mol (E_{exch}), -3.16 kJ/mol (E_{Ind}) and -6.33 kJ/mol (E_{D}).

Both central groups have similar angles, according to the stabilization energies they are weak hydrogen bonded systems. In (H_2O)-(PH_3), the stabilization energy and all basic contributions are larger than in (H_2S)-(PH_3).

7.2.2.3 Group 15

7.2.2.3.1 (PH_3)-(NH_3)

(PH_3)-(NH_3) contains a P–H bond pointing to the N atom. The P$\cdots$N distance is 4.09 Å and the P–H$\cdots$N angle is 164 °. The stabilization energy is -4.60 kJ/mol and the basic contributions are -6.34 kJ/mol (E_{elst}), 9.37 kJ/mol (E_{exch}), -2.40 kJ/mol (E_{Ind}) and -5.23 kJ/mol (E_{D}).

According to the stabilization energy, this complex has a weak HB.

7.2.2.3.2 (NH_3)-(PH_3)

(NH_3)-(PH_3) contains a N–H bond pointing to the P atom. The N$\cdots$P distance is 3.95 Å and the P–H$\cdots$N angle is 157 °. The stabilization energy is -5.40 kJ/mol and the basic contributions are -6.06 kJ/mol (E_{elst}), 6.91 kJ/mol (E_{exch}), -1.55 kJ/mol (E_{Ind}) and -4.70 kJ/mol (E_{D}).

According to the stabilization energy, this complex has a weak HB.

7.2.2.4 Group 14

The (CH_4)-(PH_3) complex has no central group with a bridging H atom. The C$\cdots$P distance is 3.77 Å. The stabilization energy is -3.18 kJ/mol and the basic contributions are -1.86 kJ/mol (E_{elst}), 5.05 kJ/mol (E_{exch}), -0.44 kJ/mol (E_{Ind}) and -5.94 kJ/mol (E_{D}).

The (SiH_4)-(PH_3) complex has no central group with a bridging H atom. The

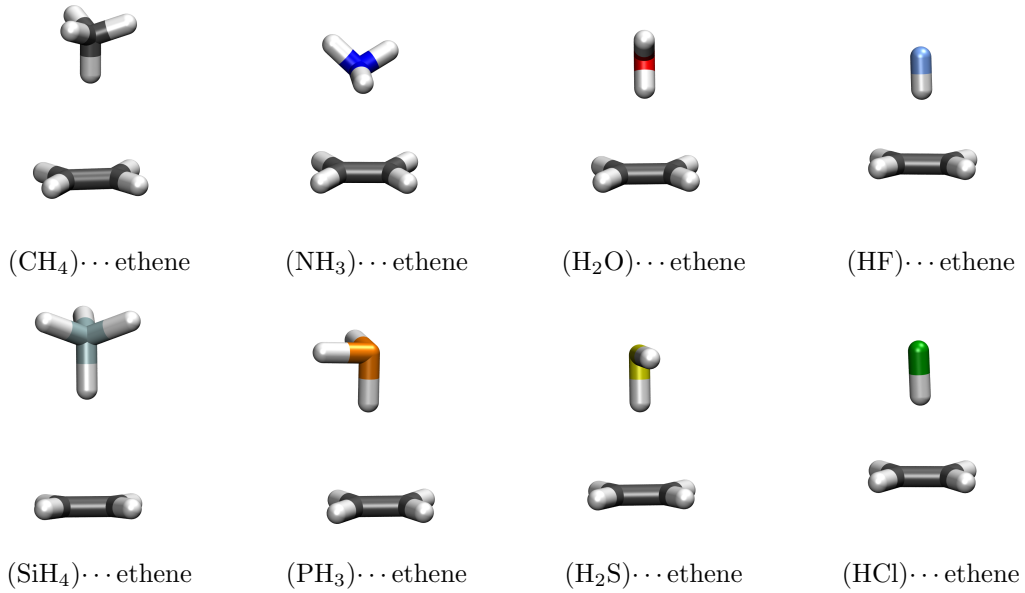

Figure 7.4: Different structures of the investigated molecules.

Si···P distance is 4.16 Å. The stabilization energy is -3.63 kJ/mol and the basic contributions are -1.92 kJ/mol (E_{elst}), 6.10 kJ/mol (E_{exch}), -0.66 kJ/mol (E_{Ind}) and -7.15 kJ/mol (E_{D}).

Neither molecule in both complexes can unambiguously be call the donor or acceptor. In both complexes, induction is unimportant, the contributions of electrostatics are less than 50 percent of exchange and dispersion, which are similar in magnitude.

7.2.3 Molecule-ethene

The acceptor molecule in the weak hydrogen bonded systems is ethene and molecules with A–H groups as donor.

Figure 7.4 shows the equilibrium structures of the studied complexes; all structures contain a hydrogen bridge. Geometry parameters and energies are given in Table 7.7.

Table 7.7: SAPT and CCSD(T) results of the different molecules interacting with ethene; the distances are measured between the heavy atom of the first molecule and the two different carbon atoms of the ethene; distances are in Å and energies are in kJ mol^{-1}.

Donor	R(X-C1)	R(X-C2)	E_{elst}	E_{exch}	E_{Ind}	E_{D}	E_{SAPT}	$E_{\text{CCSD(T)}}$
(CH_4)	4.26	4.26	-1.79	3.59	-0.53	-3.50	-2.24	-2.00
(NH_3)	3.55	3.62	-7.78	10.39	-1.68	-7.39	-6.46	-6.55
(H_2O)	3.45	3.45	-14.00	15.29	-4.95	-7.93	-11.60	-10.49
(HF)	3.16	3.13	-26.48	29.49	-14.05	-10.49	-21.53	-18.76
(SiH_4)	4.88	4.89	-0.54	2.58	-0.38	-3.06	-1.41	-1.15
(PH_3)	4.44	4.52	-2.91	5.92	-1.06	-5.06	-3.11	-2.65
(H_2S)	4.07	4.07	-8.19	11.01	-1.17	-7.62	-5.96	-6.12
(HCl)	3.73	3.70	-17.47	21.66	-9.71	-10.82	-16.34	-12.35

7.2.3.1 Group 17

(HF)-ethene contains a F–H bond orthogonal to the molecule plane of ethene with the hydrogen atom pointing to the π bond. The complex has C_{2v} symmetry. The stabilization energy is -21.53 kJ/mol and the basic contributions are -26.48 kJ/mol (E_{elst}), 29.49 kJ/mol (E_{exch}), -14.05 kJ/mol (E_{Ind}) and -10.49 kJ/mol (E_{D}).

(HCl)-ethene contains a Cl–H bond orthogonal to the molecule plane of ethene with the hydrogen atom pointing to the π bond. The symmetry is C_{2v}. The stabilization energy is -16.34 kJ/mol and the basic contributions are -17.47 kJ/mol (E_{elst}), 21.66 kJ/mol (E_{exch}), -9.71 kJ/mol (E_{Ind}) and -10.82 kJ/mol (E_{D}).

Both complexes have the same point group symmetry; the main difference is the distance between the donor molecule and ethene. According to the stabilization energies, (HCl)-ethene has a weak HB, (HF)-ethene could be classified as having a weak, moderate HB. The different stability of the two complexes is caused by

electrostatics, exchange and induction, which are all larger in (HF)-ethene; the dispersion contribution is in both complexes nearly the same.

7.2.3.2 Group 16

(H_2O)-ethene has C_s symmetry; it contains a O–H bond pointing to the π bond in ethene. The stabilization energy is -11.60 kJ/mol and the basic contributions are -14.00 kJ/mol (E_{elst}), 15.29 kJ/mol (E_{exch}), -4.95 kJ/mol (E_{Ind}) and -7.93 kJ/mol (E_D).

(H_2S)-ethene has C_s symmetry; it contains a S–H bond pointing to the π bond in ethene. The stabilization energy is -5.96 kJ/mol and the basic contributions are E_{elst} -8.19 kJ/mol, E_{exch} 11.01 kJ/mol, E_{Ind} -1.17 kJ/mol and E_D -7.62 kJ/mol.

Both complexes have weak HBs, the higher stability of (H_2O)-ethene is due to electrostatics, exchange and induction, which are all larger in (H_2O)-ethene; the dispersion contribution is in both complexes nearly the same.

7.2.3.3 Group 15

In (NH_3)-ethene no N–H bond points orthogonally to the molecule plane of ethene, the deviation from orthogonality is about 30 °. The symmetry is C_s. See Figure 7.4. The stabilization energy is -6.46 kJ/mol and the basic contributions are -7.78 kJ/mol (E_{elst}), 10.39 kJ/mol (E_{exch}), -1.68 kJ/mol (E_{Ind}) and -7.39 kJ/mol (E_D).

(PH_3)-ethene contains one P–H bond orthogonal to the molecule plane of ethene, the symmetry is C_1. The stabilization energy is -3.11 kJ/mol and the basic contributions are -2.91 kJ/mol (E_{elst}), 5.92 kJ/mol (E_{exch}), -1.06 kJ/mol (E_{Ind}) and -5.06 kJ/mol (E_D).

Both complexes have weak or very weak HBs, (PH_3)-ethene is half as stable as is (NH_3)-ethene. In both complexes the repulsive exchange outweighs the attractive contributions of electrostatics and induction, the stabilization is caused by dispersion

interaction.

7.2.3.4 Group 14

In (CH_4)-ethene a C–H bond points orthogonally to the molecule plane of ethene; the symmetry is C_1 . The stabilization energy is -2.24 kJ/mol and the basic contributions are -1.79 kJ/mol (E_{elst}), 3.59 kJ/mol (E_{exch}), -0.53 kJ/mol (E_{Ind}) and -3.50 kJ/mol (E_{D}).

In (SiH_4)-ethene a Si–H bond points orthogonally to the molecule plane of ethene; the symmetry is C_1. The stabilization energy is -1.41 kJ/mol and the basic contributions are -0.54 kJ/mol (E_{elst}), 2.58 kJ/mol (E_{exch}), -0.38 kJ/mol (E_{Ind}) and -3.06 kJ/mol (E_{D}).

Both complexes have very weak HBs, the difference between the stabilization energies is only 0.4 kJ/mol with (CH_4)-ethene being more stable than (SiH_4)-ethene, in which all basic contributions are smaller than in (CH_4)-ethene.

7.3 Discussion

All complexes containing H_2O, HF, H_2S and HCl have one central A–H$\cdots$B group. For the ammonia dimer several equilibrium structures exist that are energetically very similar,[61, 62] but we studied only a C_{s} structure with one HB and a cyclic structure of $C_{2\mathrm{h}}$ with two HBs. No bridging hydrogen atom is found in the dimers $(CH_4)_2$, $(PH_3)_2$ and $(SiH_4)_2$. The bond angles of the central group are in the range of 122 to 171 °.

It is non surprising that $(CH_4)_2$, $(PH_3)_2$ and $(SiH_4)_2$ do not have hydrogen bridges, because, based on Pauling's electronegativity scale, the C–H, P–H and Si–H bond should be nearly non-polar, the differences of electronegativities for the atom pairs (C,H), (P,H), and (Si,H) are 0.3, 0.0 and -0.3, respectively. These

differences give only a very rough impression about the corresponding bond dipole moments and therefore the tendency of forming a HB. Since the sum of all bond dipole moments is the molecular dipole moment the resulting molecular dipole of methane and silane is zero. Because of the high T_d symmetry the four bond dipole moments cancel each other out. The same is true for the quadrupole moment. In neither molecule is an acceptor atom carrying lonepairs to which a polar donor bond could point.

In phosphane with its C_{3v} symmetry, one could expect zero bond dipole moments according to the same electronegativity values of phosphorus and hydrogen, but phosphane has a small but finite molecular dipole moment of 0.57 D compared to the dipole moments of water (1.85 D) and ammonia (1.47 D).[63] Accordingly, the PH bond dipole moments should be small but finite. The structure of the stable phosphane complex demonstrates that the small polarity of the phosphane molecules and of the P–H bonds cannot stabilize a complex with a classical hydrogen bridge.

All mixed complexes containing PH_3 as donor or acceptor have a hydrogen bridge, except for CH_4 and SiH_4. In all complexes of ethene as hydrogen bond acceptor and the other molecules as donor a hydrogen bridge is found, even with CH_4 and SiH_4 as donor.

The stabilization energies of all complexes are in the range of 63 to 2 kJ/mol, complexes with stabilization energies in the range of 63 to 17 kJ/mol have, according to Jeffrey's classification, moderate hydrogen bonds, complexes with stabilization energies between 8 and 17 kJ/mol are systems with weak hydrogen bonds, and those with stabilization energies between 2 and 8 kJ/mol have very weak hydrogen bonds. Because not all complexes studied have a hydrogen bridge, we speak only of the classes of moderate, weak and very weak complexes.

In Table 7.8 the investigated molecules are colored according to their main

attractive component(s); bold black means electrostatic, turquoise dispersion and orange mixed. Main contribution means it is about 100 % or more of the total interaction energy.

The class of moderate complexes comprises $(H_2O)_2$, $(HF)_2$, (HF)-$(PH_3)_2$, (HCl)-$(PH_3)_2$ and (HF)-ethene. All of them contain a donor molecule with a pronounced molecular dipole moments and a polar donor group; the electrostatic contribution dominates. However, Figure 7.6 shows that neither induction nor dispersion is negligible, both contribute significantly.

To the class of weak complexes belong the complexes $(NH_3)_2$, $(H_2S)_2$, $(HCl)_2$, (H_2O)-(PH_3), (H_2O)-(ethene) and (HCl)-(ethene). In all of them electrostatics still dominates but the fraction of dispersion becomes large, in case of $(H_2S)_2$ and $(HCl)_2$ electrostatics and dispersion contribute nearly equally to the total interaction energy. From all ethene containing complexes only those with strong donor molecules like H_2O or HCl belong to this class.

All complexes containing CH_4, SiH_4, PH_3 and ethene are very weak complexes. The interaction in all of them is dominated by dispersion, electrostatics is extremely small in the methane and silane dimers, being smallest for the silane dimer, see Figure 7.6. This is because CH_4 and SiH_4 are non-polar molecules; the first non vanishing multipole moment in these molecules is the octopole moment. The octopole-octopole interaction is extremely short-range, it goes as r^{-7} with the intermolecular distance r. The electrostatic component in $(PH_3)_2$ is much larger than in $(CH_4)_2$ or $(SiH_4)_2$, because phosphane has a non-zero dipole moment; nevertheless, the complex does not have a hydrogen bridge. The smallest multipole moment in ethene is a quadrupole, the electrostatic contributions are accordingly small.

To find out whether there is any kind of stabilization in a complex with a hydrogen bridge, the potential energy surface for the rigid rotation of one phosphane molecule

Table 7.8: Grouped complexes into the classes according to their energy. The classes are defined as follows: moderate 17-63 kJ/mol, weak 17-8 kJ/mol and very weak 8-2 kJ/mol; colors are according to their main contribution: black (electrostatics), turquoise (dispersion) and orange (mixed, that is not a single contribution is dominant). Systems indicated by a ✓, have a hydrogen bridge.

Moderate	Weak	Very Weak
$(H_2O)_2$ -20.93 ✓	$(NH_3)_2$ -12.32 ✓	$(CH_4)_2$ -2.03
$(HF)_2$ -19.82 ✓	$(H_2S)_2$ -9.16 ✓	$(SiH_4)_2$ -2.70
	$(HCl)_2$ -10.61 ✓	$(PH_3)_2$ -5.86
(HF)-(PH_3) -23.14 ✓	(H_2O)-(PH_3) -11.54 ✓	(PH_3)-(CH_4) -3.18
(HCl)-(PH_3) -17.45 ✓		(PH_3)-(NH_3) -4.60 ✓
		(PH_3)-(H_2O) -4.43 ✓
		(PH_3)-(HF) -2.83 ✓
		(PH_3)-(SiH_4) -3.63
		(PH_3)-(H_2S) -3.33 ✓
		(PH_3)-(HCl) -2.91✓
		(NH_3)-(PH_3) -5.40 ✓
		(H_2S)-(PH_3) -7.89 ✓
(HF)-ethene -21.53 ✓	(H_2O)-ethene -11.60 ✓	(CH_4)-ethene -2.24 ✓
	(HCl)-ethene -12.35 ✓	(NH_3)-ethene -6.55 ✓
		(SiH_4)-ethene -1.15 ✓
		(PH_3)-ethene -2.65 ✓
		(H_2S)-ethene -6.12 ✓

in $(PH_3)_2$ was calculated (see Figure 7.5). The rotation was performed for different P-P distances. The rotation axis goes through the P atom of the rotating molecule and is orthogonal to the line going through the two P atoms, it is nearly coincident with a P–H bond. The equilibrium structure without a linear hydrogen bridge correspond to a rotation angle of zero degree. The interaction is repulsive for all structures with nearly linear hydrogen bridges. The origin is the strong repulsion, which outweighs the extra stabilization coming from electrostatic, induction and dispersion contribution; shown in Table 7.4.

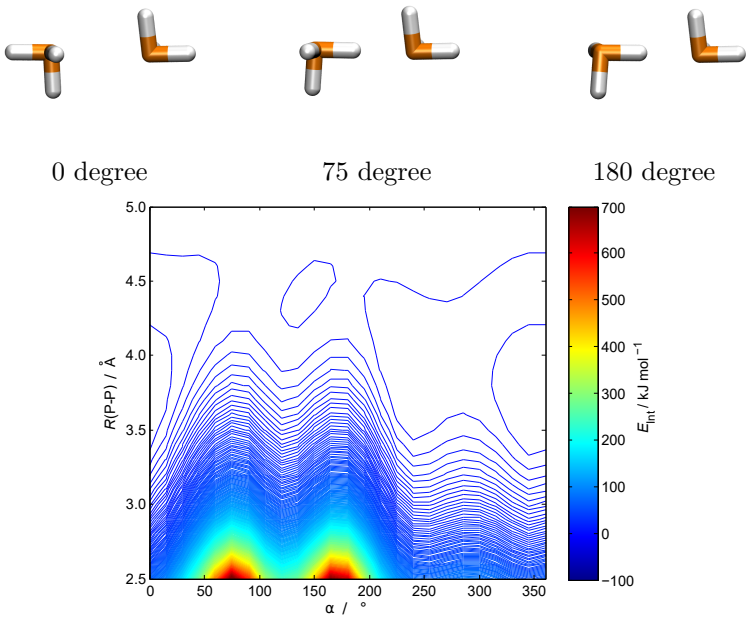

Figure 7.5: Contour plot of the energy surface (coloured) with basis set aTZ depending on the P-P distance (2.5 to 5.0 Å with step size 0.1 Å) and rotation of only one monomer in such a way that PHP group is lying in xy plane and rotating is carried out around the z axis (one full rotation in 15 ° steps). Three structures are drawn on top with angle α 0, 75 and 180 °.

In Figure 7.6, we show the contribution of the four basic interactions as multiple of the total interaction energy. In most complexes, the contribution of electrostatics

is about as large as the total interaction energy; only in very weak complexes, electrostatics is much less important than dispersion. The largest contributions are found in complexes where both molecules have non-negligible dipole moments; but also dipole-quadrupole interactions can be large, as found in complexes containing ethene. The smallest electrostatic contributions come from quadrupole-octopole, for example methane-ethene, or octopole-octopole interactions. Interactions between multipoles higher than dipole may result in unexpected equilibrium structure, as found in the (NH_3)-ethene complex, where neither the NH_3 molecule axis nor a N–H bond is normal to the ethene molecule plane (see Figure 7.4).

Induction is the smallest contribution to the total interaction energy, irrespective of the type of complex, it is seldom larger than 50 % of the total interaction energy. It becomes relatively important in interactions of a molecule with a large static dipole moment with a molecule having a polarizable electron distribution (large static polarizability) as, for example, in complexes containing hydrogen halides as polar molecules and ethene as polarizable molecule.

Dispersion interaction depends on the dynamic polarizabilities of the interacting molecules, it is independent of whether static multipoles exist or not. In weak or very weak complexes dispersion dominates the intermolecular interaction, its contribution may be twice as large as the total interaction energy, as in (SiH_4)-(PH_3) or (SiH_4)-ethene. But also in complexes where electrostatics dominates the dispersion contribution is seldom smaller than 50 % of the total interaction energy.

The exchange is the only repulsive basic interaction. In all complexes it is larger than the electrostatic contribution, in most complexes it is larger than the sum of the contributions of electrostatics and induction. Exchange repulsion increases with increasing number of interacting electrons. Equilibrium geometries are the result of the balance of attractive and repulsive interactions, therefore exchange plays a crucial role for the structure of systems without strong attractive interaction. Stone

showed in 2013 that the angular structure of halogen bonded systems is dominated by exchange repulsion. [64]

In phosphane-molecule complexes one can see how stability changes when the donor/acceptor role of the involved molecules changes. Due to the different ranges and the different strengths of the basic interactions contributing to the total interaction, any change of the distance between the heavy atoms may result in tremendous changes of the individual contributions. This can be best seen in the phosphane-HF complexes. Both (PH_3)-HF and HF-(PH_3) have hydrogen bridges but the F-P distances is in the HF-(PH_3) complex by 0.7 Å shorter than in (PH_3)-HF, all basic contributions are accordingly larger making HF-(PH_3) ten times more stable that (PH_3)-HF (see Table 7.6).

Table 7.8 shows that all moderate and all weak complexes have a hydrogen bridge; only very weak complexes may be without a hydrogen bridge. The existence of a hydrogen bridge is therefore not responsible for higher stability of a complex, from the magnitude of the stabilization energy it cannot be deduced that a hydrogen bridge exists.

There are chemists who speak of weak hydrogen bonds when a C–H acts as a hydrogen bond donor, such systems are extensively discussed in the book by Desiraju.[3] A typical example of such a system is the benzene dimer with T-shape structure or the (CH_4)-ethene complex, where C–H bonds point to π systems. Besides the T-shape structure, the benzene dimer can have a stable parallel displaced structure without a C–H bond normal to the π system. The interaction energies of these structures are in the small range from -2.7 to -2.8 kJ/mol.[65] To conclude that the dimer structure with the hydrogen bridge is stabilized because of (very) weak hydrogen bonding, is at least questionable. It completely ignores the stabilization of these structures due to the interaction of the benzene quadrupoles.[16]

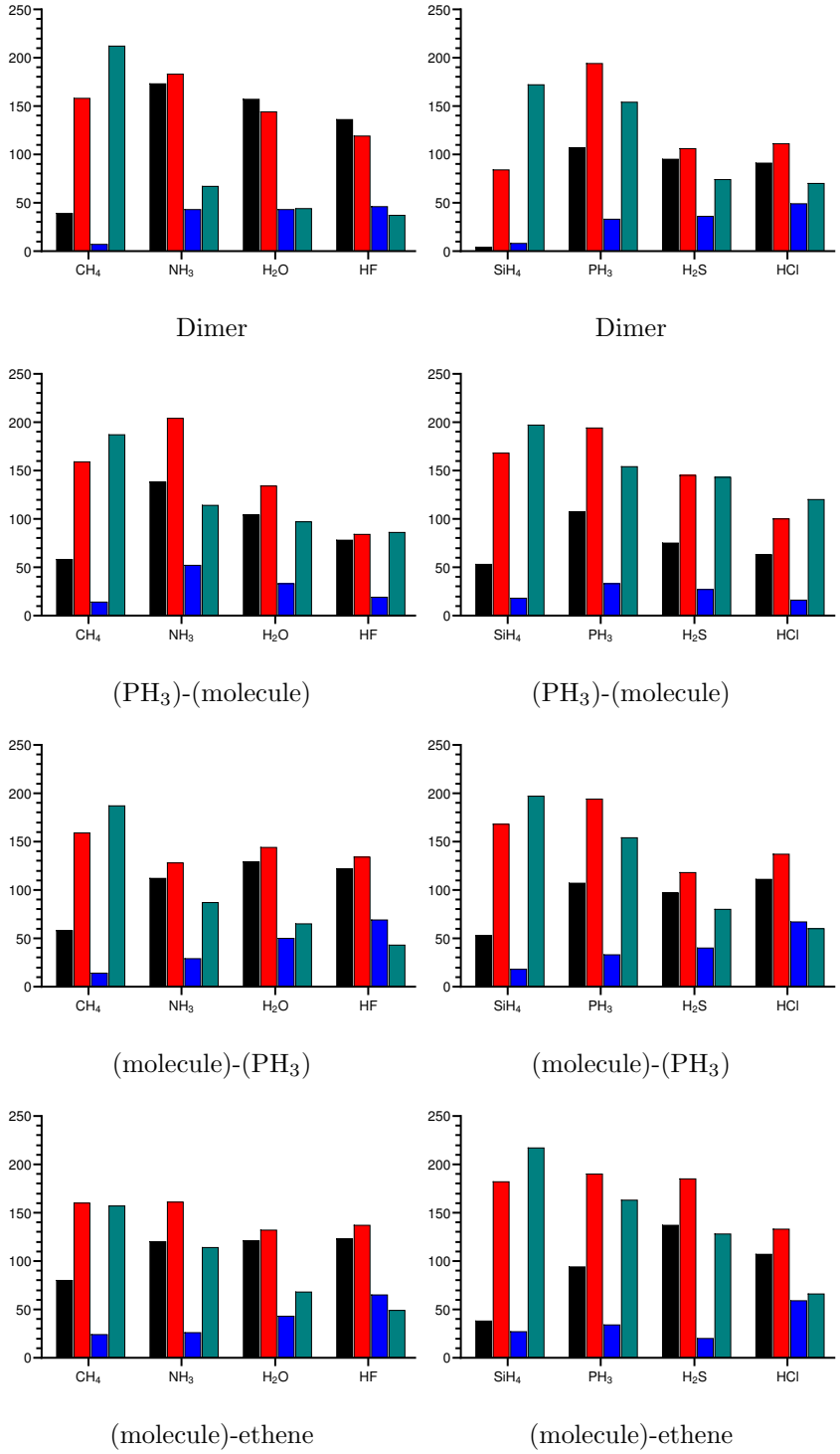

Figure 7.6: Absolute percentage of the components in the various complexes (only NH_3 dimer with one hydrogen bond); coloured E_{elst} **black**, E_{exch} **red**, E_{Ind} **blue** and E_{D} **turquoise**. Left: first period, right: second period.

The distance dependence of the total interaction energy and the basic components (Figures 7.7 and in Appendix A.2) shows a great difference between systems containing first and second row atoms. The energy curves from the second row are shifted to more positive values and the curvatures at the local minima are much smaller than for the first-row curves. The curves for $(CH_4)_2$ and $(SiH_4)_2$ become identical at $R_{red} \approx 1$ with $(SiH_4)_2$ being slightly more stable (Figure 7.7A), for the other system pairs this is found for much larger R_{red} values. On the other hand, there is great similarity of the curves of the water and HF dimers and of $(H_2S)_2$ and $(HCl)_2$. For the dispersionless interaction energies (Figure 7.7B), the similarities are even greater. Figure A.2 in the Appendix shows that the similarity of the interaction energies for $(CH_4)_2$ and $(SiH_4)_2$ is due to the similarities of the basic components.

Without dispersion contributions, interaction energies are smaller and the intermolecular distances are longer (see Figure 7.7B). This was also found in the work from Hoja and Sax for alcohol dimers.[66]

For all second period dimers the minimum, which should be at $R_{red} = 1$ is at around $R_{red} = 0.95$. The reason could be that the methods the geometry optimization and for the calculation of the interaction energies are not the same.

Finally, Figure A.2) in Appendix shows that no basic interaction component can explain equilibrium structures because as a function of the intermolecular distance, none of them has a local minimum. Only the sum of attractive and repulsive contributions can explain the geometry of stable structures. But since the sum of electrostatics, induction and exchange frequently cancels, any explanation of stable structures without considering dispersion interaction fails.

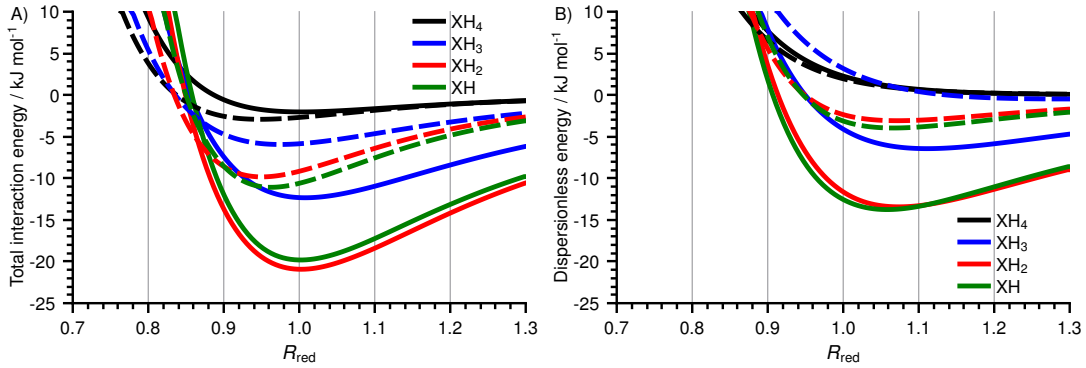

Figure 7.7: A) Total interaction curves and B) dispersionless curves for with hydrogen atoms saturated main group dimers; first period solid line, second period dashed line

8 The special case of amines

8.1 Methods

The dispersionless DF, dlDF,[67] was designed to reproduce for interacting systems the dispersionless interaction energy defined as the difference of coupled-cluster interaction energies and the dispersion contributions to the interaction energy calculated with SAPT(DFT).[56, 68] The dispersion contribution to the total interaction energy, D_{as}, is calculated as the sum of contributions from atom pairs, where each of the two interacting molecules contributes one atom (intermolecular atom pairs).[69] The parameters describing the atomic contributions were fitted against the SAPT(DFT)/CBS energies. The sum of dlDF and D_{as} is denoted as dlDF+D_{as}. Whether conventional Kohn-Sham or hybrid DFs cover a certain amount of dispersion energy cannot be answered with certainty. Interaction energies calculated in a supermolecular approach using such methods may yield a very good agreement with results from high-quality methods, but this agreement could be fortuitous. Manifest shortcomings of such DFs can be cured with empirical correction schemes. For several systems, we compared dlDF+D_{as} results with these obtained with B3LYP [48] and Grimme's D2 and D3 dispersion correction,[49, 70] these methods are labelled B3LYP+D2 and B3LYP+D3, respectively. Both D_{as} and Grimme's D2 and D3 corrections are basis set independent. For some structures of the cyclic ammonia dimer and the methylamine dimer, taken from the BEGDB

data base,[46] we compared DFT energies with CCSD(T) energies obtained at the complete basis set limit (CBS).

For the basis set studies, we used Dunning's basis sets and their former introduced abbreviations. Geometry optimization of amine dimers was performed with the DZ basis set. The usual method/basis notation is used throughout in this work. All interaction energies and gradients were corrected for the basis set superposition error by using the counterpoise correction method by Boys and Bernardi.[38]

The DFT calculations were performed with NWChem 6.2[71], gradients for dlDF+D_{as} were implemented in a local copy of this program system.

Start geometries were created with Avogadro.[47]

8.2 Investigated systems

In this study, we investigate the parent ammonia dimer $(NH_3)_2$ and the homomolecular dimers of primary amines with the following linear and branched alkyl groups: methyl (Me), ethyl (Et), *n*-propyl (*n*Pr), *n*-butyl (*n*Bu), *iso*-propyl (*i*Pr) and *tert*-butyl (*t*Bu). This allows to study the influence of shape and size of the substituents on the dimer properties. In the following, amine dimers are denoted just by the name of the alkyl group, e.g., Me_2 instead of $(MeNH_2)_2$, iPr_2 instead of $(i\mathrm{PrNH}_2)_2$ etc.

As mentioned in the first part of this work several structures for the ammonia dimer exist, but we investigated only two C_s structures with a single HB, denoted staggered and eclipsed, and a cyclic one with two HBs (see Figure 8.1). The eclipsed structure corresponds always to a local minimum on the potential energy surface and the staggered structure corresponds, basis set dependent, to either a local minimum or to a saddle point; therefore we used only the eclipsed structure for comparison of cyclic and non-cyclic ammonia dimers and for the construction of the

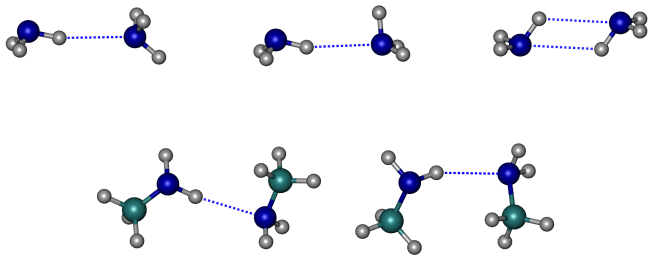

Figure 8.1: First row: Equilibrium structures of staggered (left), eclipsed (middle), cyclic (right) $(NH_3)_2$. Second row: Equilibrium geometries of *cis*-Me_2 (left) and *trans*-Me_2 (right).

amine dimers. All amine dimers are connected by a single HB; the structures with linear alkyl groups (see Figure 8.2) were obtained in the following way. Starting from the eclipsed ammonia dimer, the most distant hydrogen atoms were substituted by methyl groups followed by unconstrained geometry optimization by using dlDF+D_{as}. Then, the most distant hydrogen atoms were replaced by methyl groups and the structure optimized, and so on. This gave a group of dimers with most distant terminal methyl groups, called the *trans* group. The created alkyl groups are in an all-antiperiplanar conformation. This is also the way the alcohol dimers it were constructed in another SAPT(DFT) study.[66] By using a different start geometry, we found another group of structures, called *zigzag*, which differ from the *trans* structures mainly by the angular structure of the central moiety.

When in the methyl groups of the dimethylamine dimer Me_2 the hydrogen atoms that are closest together are replaced by methyl groups, one gets the *cis* group of dimers; roughly speaking, the substituents are aligned parallel. In dimers with large substituents, two different alignments of the alkyl chains are possible, which we call *syn* and *anti*. (See Figure 8.3.) We also investigated a small number of structures where the alkyl groups are partially in clinal conformations. Discussion of *cis* dimers is always based on the *anti* structures.

Zigzag structures correspond to local minima only at the dlDF+D_{as} level; opti-

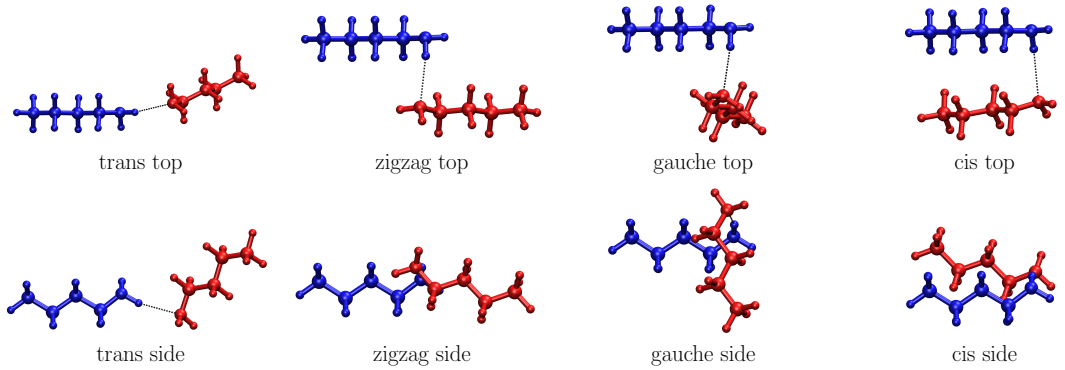

Figure 8.2: Top and side views of the four nBu$_2$ isomers.

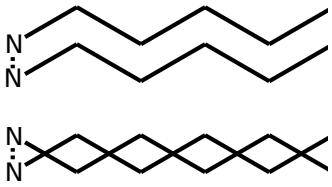

Figure 8.3: *Syn* (Top) and *anti* (bottom) arrangement of the alkyl chains in *cis* dimers. The alkyl groups are in the all-antiperiplanar conformation.

mization with B3LYP+D2 and B3LYP+D3 leads immediately to the more stable *gauche* structures, which are, somehow, in between the most stable *cis* and the unstable *zigzag* structures. For the small dimer Me_2, there is no difference between *cis* and *gauche*.

The fourth group consists of the amines with branched substituents; this group can be considered as being derived from Me_2 by successively replacing the methyl hydrogen atoms by methyl groups. Structures derived from the parent *trans*-Me_2 are labelled I, these derived from *cis*-$MeNH_2$ are labelled II.

8.3 Comparison of methods

Before using the dlDF+D_{as} method we need to validate it. First, we study the basis set dependence of the three methods dlDF+D_{as}, B3LYP+D2 and B3LYP+D3 and the influence of the dispersion energy or dispersion correction on the stabilization energies for the equilibrium structures of the non-cyclic and the cyclic ammonia dimers and *cis*-Me_2 and *trans*-Me_2. The equilibrium structures of the cyclic ammonia dimer[65] and of *cis*-Me_2[72] are taken from the BEGDB data base,[46] the eclipsed, non-cyclic ammonia dimer was optimized with the TZ basis and *trans*-Me_2 was optimized with the DZ basis. Next, we compare the shapes of the potential curves for the rigid dissociation of the ammonia dimer and the methylamine dimer using the three methods. Finally, we compare the equilibrium structures obtained by unconstrained optimization. For this comparison, we calculated equilibrium geometries of the two ammonia dimers and of all amine dimers.

8.3.1 Basis sets

For the investigation of the basis set dependence we need only the dlDF and B3LYP energies given in Table 8.1. The energies including dispersion contributions are given in the Appendix. The stabilization energies shown in Figure 8.4 demonstrate in addition the influence of the dispersion contributions on the stabilization energies. We find for all systems and with both functionals: 1) convergence of the stabilization energies at the quintuple zeta level; and 2) that a5Z and 5Z values are essentially equal. We find that for the Me_2 dimers the a5Z values are larger by about 0.02 kJ/mol than the 5Z values, for the ammonia dimers the a5Z values are smaller than the 5Z values by 0.01 kJ/mol for the non-cyclic and 0.07 kJ/mol for the cyclic dimer. We find uniform convergence behaviour for the Me_2 dimers, but different convergence for the ammonia dimers, depending on the basis set type (augmented

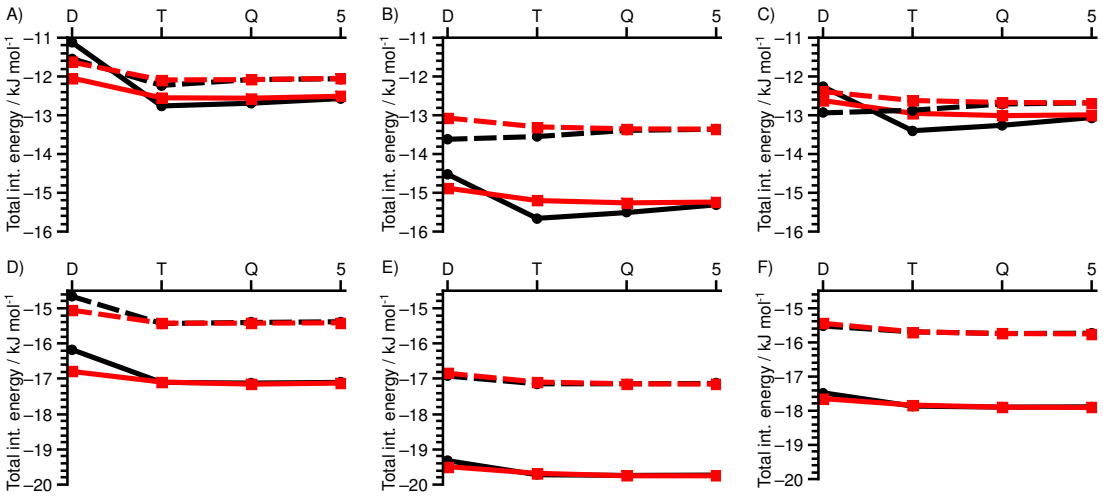

Figure 8.4: Basis set study of the stabilization energy (total interaction energy) with the density functional based methods dlDF A) and D), B3LYP+D2 B) and E) and B3LYP+D3 C) and F): A) - C) ammonia dimer with two differet geometries, where full line is the cyclic structure with two HBs from BEGDB and dashed correspond to the non cyclic with one HB; and D) - F) Me_2 with *cis* (full lines), geomtry from BEGDB, and trand geometry (dashed lines); augmented aXZ (red) and unaugmented XZ (black) basis sets from Dunning with X=D,T,Q,5 are used.

Table 8.1: Basis set dependence of $(NH_3)_2$ with 1 HB and 2 HB and Me_2 *trans* and *cis*

	$(NH_3)_2$ 1 HB		$(NH_3)_2$ 2 HB		*trans*-Me_2		*cis*-Me_2	
Basis	dlDF	B3LYP	dlDF	B3LYP	dlDF	B3LYP	dlDF	B3LYP
DZ	-4.55	-9.68	-1.85	-8.43	-0.73	-8.40	+0.18	-8.59
TZ	-5.24	-9.61	-3.49	-9.57	-1.50	-8.62	-0.75	-8.99
QZ	-5.09	-9.45	-3.42	-9.42	-1.47	-8.62	-0.77	-9.01
5Z	-5.07	-9.42	-3.30	-9.22	-1.45	-8.61	-0.75	-9.00
aDZ	-4.64	-9.13	-2.77	-8.79	-1.12	-8.32	-0.44	-8.76
aTZ	-5.10	-9.36	-3.28	-9.11	-1.49	-8.57	-0.74	-8.95
aQZ	-5.09	-9.41	-3.29	-9.17	-1.49	-8.62	-0.80	-9.02
a5Z	-5.06	-9.42	-3.24	-9.15	-1.48	-8.63	-0.77	-9.02

or unaugmented) and the dimer structure (cyclic or non-cyclic). For both Me_2 dimers the stabilization energies are essentially converged at the TZ level with both augmented and unaugmented basis sets, frequently the TZ and the 5Z values are identical and the QZ values are slightly (0.01 kJ/mol) larger. This is found for both functionals. The maximum differences between TZ, QZ and 5Z values are not larger than 0.07 kJ/mol for both dimers, both DFs and both types of basis sets.

The basis set convergence for the two ammonia dimers is very different for the two DFs. With dlDF and unaugmented basis sets, we observe for both dimers a strong increase of the stabilization energy when going from DZ to TZ and then a monotonic decrease to 5Z, the maximum variation is for the non-cyclic dimer, which is roughly three times as large as for the cyclic dimer. With augmented basis sets, the variations are smaller and the aTZ values are essentially equal to the a5Z values. With B3LYP we find for the cyclic dimer essentially the same convergence as with dlDF but for the non-cyclic dimer we find with unaugmented basis sets

a monotonic decrease and with augmented basis sets a monotonic increase of the stabilization energies. As for the Me_2 dimers, the 5Z and a5Z energies are essentially equal, and the aTZ energies are very close to the a5Z values.

The different convergence of the counterpoise corrected stabilization energies shows the need of large basis sets for small systems like the ammonia dimers, whereas in the Me_2 dimers the additional basis sets from the methyl groups augment the basis and, therefore, the small unaugmented basis set TZ is sufficient to get reliable stabilization energies. TZ is therefore the basis of choice for calculating the stabilization energy in amine dimers. For the ammonia dimers, we need at least the aTZ basis set or the QZ basis set.

8.3.2 Dispersion method

The differences between the basis set limits obtained for the three methods are caused by the different energies calculated with the DFs and the different contributions of dispersion interaction to the stabilization energy. This is what we find: for the non-cyclic ammonia dimer, the dispersion contributions are -6.99 kJ/mol (D_{as}), -3.94 kJ/mol (D2) and -3.26 kJ/mol (D3), for the cyclic dimer the respective values are -9.27 kJ/mol, -6.09 kJ/mol and -3.84 kJ/mol. When these dispersion contributions are added to the pure DFT a5Z energies we get for the non-cyclic dimer stabilization energies of -12.05 kJ/mol, -13.36 kJ/mol and -12.68 kJ/mol and for the cyclic dimer -12.51 kJ/mol, -15.24 kJ/mol and -12.99 kJ/mol, respectively. Comparison with the CCSD(T)/CBS value of -13.14 kJ/mol for the cyclic ammonia dimer shows that dlDF+D_{as} and B3LYP+D3 underestimate this value by -4.8% and -1.1%, whereas B3LYP+D2 overestimates it by 16.0%. By using these values we find for the relative stabilities of the two dimers -0.46 kJ/mol, -1.88 kJ/mol and -0.31 kJ/mol, respectively. The smallest difference between the cyclic and the non-cyclic dimer is found with B3LYP+D3, the dlDF+D_{as} value is about 50%

larger and the B3LYP+D2 is about six times larger.

The trend is similar for the Me_2 dimers. For *trans*-Me_2 the dispersion contributions are -13.93 kJ/mol (D_{as}), -8.52 kJ/mol (D2) and -7.13 kJ/mol (D3), and for *cis*-Me_2 they are
-16.35 kJ/mol, -10.73 kJ/mol and -8.88 kJ/mol, respectively. As for the ammonia dimers we find that the D_{as} values are about twice as large as the D3 corrections and that the D2 corrections are considerably larger than the D3 corrections. Adding the dispersion contributions to the pure a5Z energies gives the following stabilization energies: -15.41 kJ/mol, -17.15 kJ/mol and -15.76 kJ/mol, respectively, and -17.12 kJ/mol, -19.75 kJ/mol and -17.91 kJ/mol, for *cis*-Me_2, respectively. The dlDF+D_{as} energies are 0.35 kJ/mol and 0.79 kJ/mol smaller than the B3LYP+D3 energies. Comparison with the CCSD(T)/CBS value of -17.36 kJ/mol for *cis*-Me_2 shows that dlDF+D_{as} underestimates it by -1.4% and B3LYP+D3 overestimates it by $+3.2\%$. We do not know, however, whether for larger dimers this trend continues and both DFT methods will overestimate the CCSD(T)/CBS values. The relative stabilities of the Me_2 dimers are -1.71 kJ/mol, -2.60 kJ/mol and -2.15 kJ/mol, respectively. These rather small energy differences are composed of differences in the DFT energies and the dispersion contributions. With dlDF, *cis*-Me_2 is by 0.71 kJ/mol less stable than *trans*-Me_2, but the difference in the dispersion energy of -2.42 kJ/mol causes the higher stability of the *cis* dimer. With B3LYP, *cis*-Me_2 is more stable than *trans*-Me_2 by 0.39 kJ/mol and with the D3 contribution *cis*-Me_2 is stabilized by additional 1.75 kJ/mol.

8.3.3 Potential energy curves

The BEGDB data base contains information for rigid dissociation of cyclic $(NH_3)_2$ and *cis*-Me_2. The potential energy curves are represented by the CCSD(T)/CBS interaction energies for supporting structures as functions of the monomer distances

R, which is for $(NH_3)_2$ the H$\cdots$N distance and for Me_2 it is the distance between the centers of mass of the two monomers. The monomer distances are given in reduced units R_{red}, that is ratios of the actual monomer distance and the equilibrium distance. For the dissociation of the amine dimer five supporting structures with reduced distances R_{red} vof 0.9, 1., 1.2, 1.5 and 2 are listed, and eight supporting structures with distance values of 0.9, 0.95, 1., 1.05, 1.1, 1.25, 1.5 and 2 for the dissociation of Me_2. We calculated for these structures the interaction energies with all DFT methods, for the ammonia dimer and for Me_2 we used the aTZ basis. The eight supporting structures for the Me_2 dissociation are sufficient to get smooth curves even for these methods having their minimum not at $R_{red} = 1$; for the dissociation of the ammonia dimer, the five supporting structures give smooth curves for dlDF+D_{as} and B3LYP+D3, but for all other methods the five structures from the BEGDB data base are not sufficient, so we added three more supporting structures with R_{red} values of 0.95, 1.05 and 1.10.

Figure 8.5 shows the curves of the DFT interaction energies with and without dispersion contributions and the CCSD(T)/CBS reference curve. We see that the agreement of the dlDF+D_{as}, B3LYP+D3 and CCSD(T)/CBS curves is excellent, this is true not only for the position of the local minima and the depths of the potential well but also for the shape of the whole curves (see Figure 8.5). With B3LYP+D2, the potential wells is too deep and the local minima are shifted to smaller values of the monomer distances.

As the dlDF curves show, the sum of repulsive exchange and attractive electrostatics and induction can reproduce neither the equilibrium geometry nor the depth of the potential well as the local minima are shifted toward larger distances between the monomers and the depths of the local minima are only a fraction of the real stabilization energies. If the missing dispersion interaction is accounted for by adding D_{as} to dlDF we get the excellent agreement with the CCSD(T)/CBS

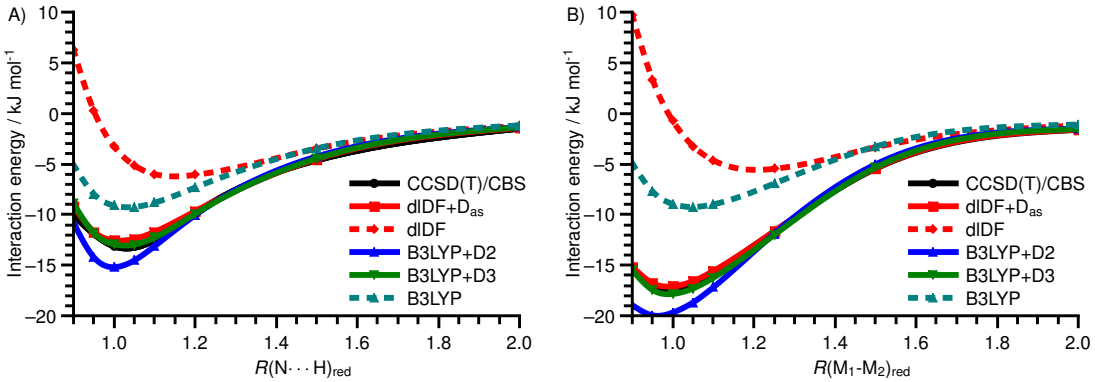

Figure 8.5: Potential curve (without relaxation of the monomer geometries) with the different methods with and without dispersion correction. A) $(NH_3)_2$, B) Me_2.

curve.

In the B3LYP curves the position of the local minima is shifted to smaller distances and the depth of the wells is increased. But only when the D3 correction is added to the B3LYP curves the positions and the values at the local minima agree with the CCSD(T)/CBS results. It is tempting to assume that this is caused by a larger amount of short or medium ranged dispersion interaction covered by the B3LYP DF, but we resist this temptation for the reasons mentioned above. We might note, in passing, that we obtained similar results also for six other semilocal DFs (Guttmann, Sax, unpublished results) making this interpretation more plausible but still not logically correct.

The dlDF curves in Figure 8.5 show also that substitution of two hydrogen atoms in the ammonia dimer by methyl groups 1) increases the steepness of the repulsive branch of the dlDF energy curve, 2) decreases the depth of the potential well and 3) shifts the position of the minimum to larger distances. From our SAPT study[66] we know that with the increase of the number of atoms in the interacting monomers all four interactions components increase in magnitude, but because the increase of exchange repulsion outweighs the increase of attractive electrostatics

and induction, exchange is responsible for the destabilization of the dimer. It is the attractive dispersion contribution that shifts the minimum of the potential well back to smaller values and increases the well depth.

8.3.4 Equilibrium geometries of dimers

We know that the TZ basis is sufficient to get reliable stabilization energies for the Me_2 dimers but that the aTZ basis is necessary for the ammonia dimers. To check the influence of basis sets on the equilibrium geometries of the ammonia and the Me_2 dimers, we performed unconstrained geometry optimizations of these structures by using the DZ and TZ basis sets. For the Me_2 isomers, we find that DZ and TZ yield very similar geometry parameters. (Guttmann, Sax unpublished)

For the ammonia dimers we find a strong influence of the basis set and the start geometry on the equilibrium structures. With dlDF+D_{as} and DZ, the staggered structure is a local minimum but with TZ it is a saddle point; with B3LYP+D3 it is the other way around. This is the reason why we concentrate only on the eclipsed structure. With the DZ basis and a slightly deformed eclipsed starting geometry all methods found the eclipsed equilibrium structure; with the TZ basis dlDF+D_{as} and B3LYP+D2 converged to the cyclic and only B3LYP+D3 converged to the eclipsed equilibrium structure. The cyclic structure was retained during a reoptimization with the smaller DZ basis. Only when the cyclic equilibrium structure obtained with dlDF+D_{as} was used as start geometry, did B3LYP+D3 with the TZ basis also find a cyclic equilibrium geometry. These findings suggest that the topography of the hypersurfaces for the ammonia dimer is dominated by several local minima of similar depth, which are not separated by large energy barriers and the stabilization energies, calculated with the aTZ basis (see Table 8.2), support this assumption. However, we did not check this assumption in detail.

For the geometry parameters we find reasonable agreement between all three

Table 8.2: Total interaction energies (aTZ basis) for cyclic and non-cyclic $(NH_3)_2$ structures optimized with DZ and TZ.

	dlDF+D_{as}		B3LYP+D2		B3LYP+D3	
	DZ	TZ	DZ	TZ	DZ	TZ
non-cyclic	-12.09	—	-14.03	—	-13.31	-13.45
cyclic	-12.26	-12.38	-15.00	-15.28	—	-13.11

methods as Table A.5 in the Appendix shows; dlDF+D_{as} yields shorter NH bonds than B3LYP, and a longer H$\cdots$N distance; the N-N distance and the NHN bond angle are again very similar.

We calculated also for the eclipsed, non-cyclic equilibrium structures the stabilization energies with basis sets up to 5Z and found the same trends as for the cyclic ammonia dimer described above. The stabilization energies of non-cyclic structures are, as expected, slightly smaller than these of cyclic structures, all energies are given in Table A.2 in the Appendix.

8.4 Structure and stability of amine dimers

Geometry optimization of all amine dimers was done with the methods dlDF+D_{as} and B3LYP+D3 using basis set DZ. Stabilization energies were calculated only with dlDF+D_{as} and the TZ basis, for the discussion of the results we use only the dlDF+D_{as} data.

8.4.1 Optimized structures

We calculated equilibrium structures of all *trans*, *cis* and *gauche* amine dimers, as well as of amines with branched substituents. The great similarity of the

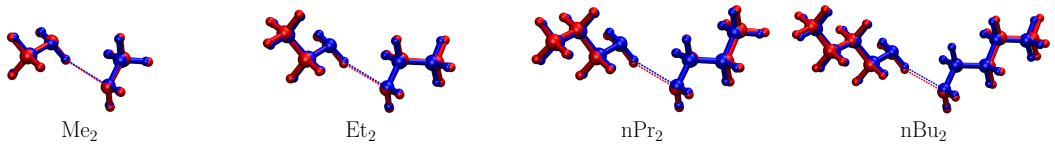

Figure 8.6: Overlay of *trans* structures obtained with dlDF+D_{as} (blue) and B3LYP+D3 (red).

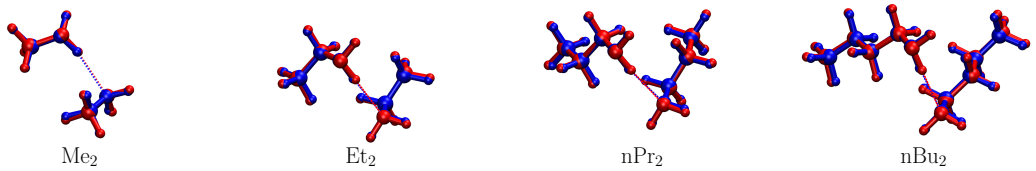

Figure 8.7: Overlay of *gauche* structures obtained with dlDF+D_{as} (blue) and B3LYP+D3 (red).

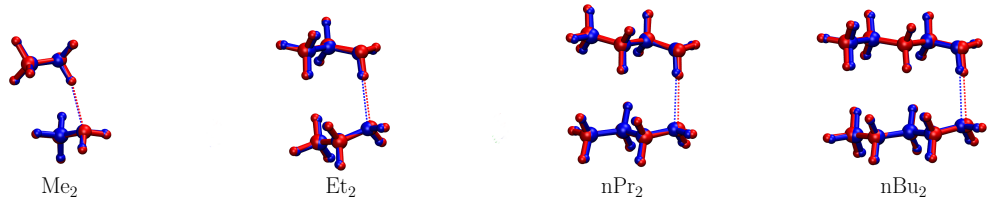

Figure 8.8: Overlay of *cis-anti* structures obtained with dlDF+D_{as} (blue) and B3LYP+D3 (red).

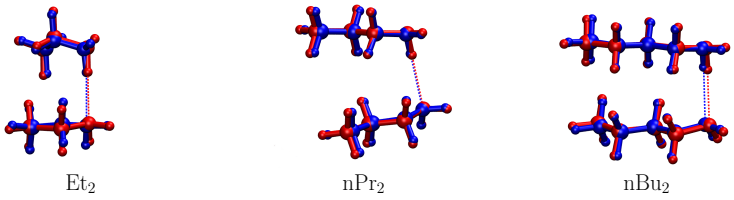

Figure 8.9: Overlay of *cis-syn* structures obtained with dlDF+D_{as} (blue) and B3LYP+D3 (red).

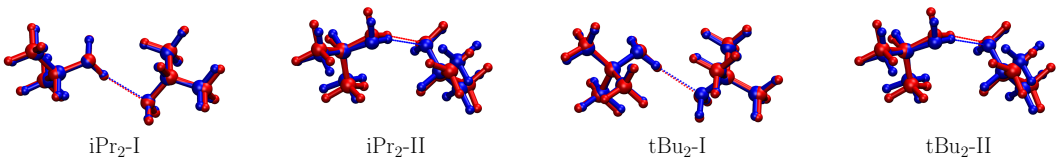

Figure 8.10: Overlay of branched structures obtained with dlDF+D_{as} (blue) and B3LYP+D3 (red).

equilibrium geometries obtained with dlDF+D_{as} and B3LYP+D3 are shown by overlays presented in Figures 8.6 to 8.10. The overlay was done with respect to the two nitrogen atoms and the two corresponding C_α atoms. All dimers are chiral molecules with the possibility of different signs for the dihedral angles C_α-N-N-C_α after geometry optimization. In the tables, all dihedral angles have positive sign. More geometry parameters can be found in the Appendix Table A.5 to A.7.

There are no tremendous differences between the geometry parameters of the central moieties (see Table 8.3 and 8.4). Whereas the N-H distance is in all dimers 0.98 Å the H$\cdots$N distance varies between 2.25 and 2.37 Å; the short distances are found for *trans* and *gauche* structures, the large values are found for the *cis* dimers with the largest substituents *n*Pr and *n*Bu. The N-N distance varies between 3.19 and 3.35 Å, again the largest distances are found in *cis* dimers with the largest substituents; the N-H$\cdots$N angle varies between 161 and 176 deg, the smaller values are found in *trans* and *gauche* dimers, larger ones in *cis* dimers.

In *trans* dimers the values of the C_α-N-N-C_α dihedral angle are rather uniform, but in *gauche* and *cis* dimers the value depends on the size of the substituents; with increasing size of the substituents the dihedral angles become similar. The distance between the terminal carbon atoms, C_ω-C_ω, can be used as a rough measure of the distance between the substituents. In *cis* dimers this distance varies between 3.81 Å for Me_2 and 4.60 Å for *syn* Pr_2; in *gauche* dimers, between 4.62 and 5.33 Å; for the branched dimers this distance is not well defined and has no meaning. The

Table 8.3: Equilibrium geometry of dimers with non-branched substituents. Distances in Å, bond angles in degrees. τ is the $C_\alpha NNC_\alpha$ dihedral angle.

	trans				*gauche*				*cis-anti*			
System	N-N	H···N	NHN	τ	N-N	H···N	NHN	τ	N-N	H···N	NHN	τ
Me_2	3.21	2.25	164	176	3.19	2.26	161	71	3.20	2.26	161	71
Et_2	3.20	2.25	164	175	3.28	2.34	162	35	3.31	2.33	176	15
nPr_2	3.19	2.25	162	172	3.29	2.35	161	29	3.35	2.37	172	26
nBu_2	3.19	2.25	162	172	3.30	2.36	161	29	3.35	2.37	173	31

Table 8.4: Equilibrium geometry of dimers with branched substituents. Distances in Å, bond angles in degrees. τ is the $C_\alpha NNC_\alpha$ dihedral angle.

System	N-N	H···N	NHN	τ
iPr_2 I	3.20	2.25	164	180
iPr_2 II	3.21	2.25	166	109
tBu_2 I	3.27	2.30	172	135
tBu_2 II	3.31	2.35	166	80

smaller distances in the *cis* series are expected because the alkyl chains grow in parallel and attract each other; in the *gauche* series an increase of alkyl chains is accompanied by a decrease of the distance between the terminal C atoms owing to the higher torsional flexibility of the substituents, together with large changes of the C_α-N-N-C_α dihedral angle. In the *trans* series, the distances between the terminal carbon atoms increase monotonically with increasing size of the substituents.

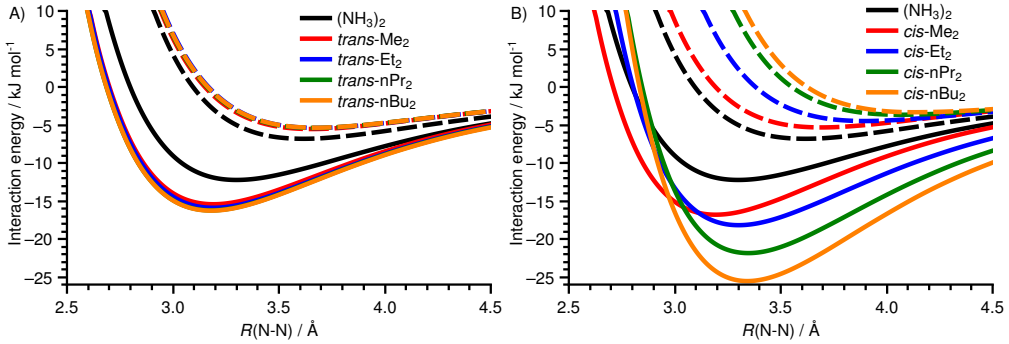

Figure 8.11: Total interaction energies (solid lines) and dispersionless interaction energies (dashed lines); A) *trans* series, B) *cis-anti* series

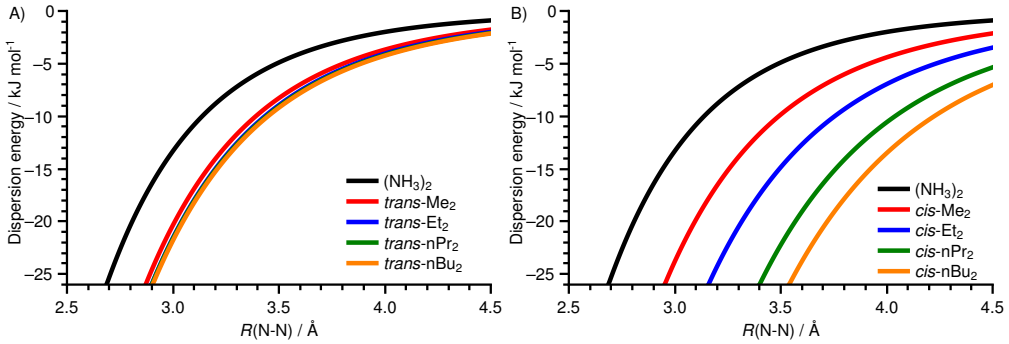

Figure 8.12: Dispersion contribution of A) *trans* and B) *cis-anti* series

8.4.2 Dissociation of amine dimers

For *trans* dimers the difference between rigid and relaxed dissociation will be minimal. It will be larger for *gauche* dimers with large alkyl chains as substituents.

Figure 8.11 shows the total interaction energies and the dispersionless interaction energies as function of the N-N distance for *trans* and *cis* dimers with *anti* alignment. In the *trans* series, the total interaction energy at the corresponding equilibrium structures increases by 3 kJ/mol when a hydrogen atom in ammonia is substituted by a methyl group, (-12.2 kJ/mol for $(NH_3)_2$ to -15.4 kJ/mol for Me_2) and the position of the local minimum decreases from 3.3 Å to 3.2 Å, but further increase of the substituents does not change significantly the stabilization energy and

the position of the minimum. The opposite trend is found for the curves of the dispersionless interaction energy, where substitution reduces the stabilization energy by 1.3 kJ/mol and shifts the minimum of the potential to larger values. Again, further increase of the substituents yields little changes in the stabilization energy and the position of the minimum. Both families of energy curves converge rapidly to a limiting curve. Convergence of the curves of the dispersionless and the total interaction energy implies also convergence of the dispersion energy curves; Figure 8.12 confirms this.

In the *cis-anti* series, there is no convergence in all three families of interaction curves. The total interaction energy increases by 4.6 kJ/mol when going from the ammonia dimer to the methylamine dimer and the position of the minimum is shifted to 3.2 Å, as in the *trans* series. Further substitutions increase the total interaction energy by 1.4 kJ/mol, 3.7 kJ/mol and 3.6 kJ/mol and shift the positions of the minima further to larger values (Table 8.5). There is no evidence for a convergence of the stabilization energies with growing substituents but the minima seem to converge to the distance of the Bu_2 dimer. For the dispersionless interaction energy, we find a monotonic reduction of the well depth and a shift of the distance where the repulsive branch becomes zero to larger values. As expected, there is no convergence of the dispersion energy curves either. (See Figure 8.12.) The interaction energies of the *syn* dimers (see Appendix) are smaller but show the same convergence behaviour. Irrespective of the large differences in the shapes of *trans* and *cis* curves, they both show that the sum of repulsive exchange repulsion, attractive electrostatic, and induction does not correctly describe the equilibrium distance of the amine complexes and the amount of stabilization. Indeed, at the respective minima of the total interaction energy, the dispersionless interaction energy is close to zero or even positive.

8.4.3 Energy components to the stabilization energy

The analysis of the stabilization energies in Table 8.5 at the respective equilibrium distances shows the influence of the size and relative orientation of the substituents on the dimer stability. For all amine dimers with linear substituents, the *trans* structures are least stable. For substituents up to nPr, the *gauche* structures are more stable than the corresponding *cis* structures, for nBu_2 the order is reversed, and we expect for all larger n-alkyl substituents that this trend continues. For iPr_2, structure II (derived from *cis*-Me_2) is more stable than structure I (derived from *trans*-Me_2), for tBu_2 it is the other way around. Structures and energies of the dimers with branched substituents are given in the Appendix.

The stabilization of *trans*-Me_2 by 3.2 kJ/mol with respect to the ammonia dimer is caused by a strong increase of dispersion interaction (7.1 kJ/mol) and a destabilization owing to a moderate decrease (3.2 kJ/mol) of the attractive dispersionless interaction. Comparison of the energy contributions to the stabilization energies of *trans* and *cis*-Me_2 shows that in the latter the smaller distance between the methyl groups decreases the still stabilizing dispersionless interaction by 1.0 kJ/mol but increases the stabilization as a result of dispersion interaction by 2.4 kJ/mol, making *cis*-Me_2 by 1.4 kJ/mol more stable than *trans*-Me_2. This trend continues in the *cis* series, the increasing destabilization owing to the dispersionless interaction energy is outweighed by the much stronger increase of the stabilizing dispersion interaction. With the growing size of the substituents, the stabilization energy quickly converges to a constant value as do the dispersion contribution and the dispersionless interaction energy. With increasing size of the substituents ,the percentage of dispersion interaction gets larger: in the ammonia dimer it is 59%, in Me_2 it is already 93% and in Bu_2 it is 95% of the stabilization energy. The dispersionless stabilization energy is small but still negative.

In both the *gauche* and the *cis* series the stabilization energies do not converge

but increase monotonically, as do the dispersionless energy and the dispersion energy. In all *cis* dimers, starting with Et_2, the dispersionless interaction energy is positive, thus destabilizing. For the Me_2 dimer, the *anti* and *syn* geometries are identical and moreover, equal to the *gauche* geometry. *Cis* dimers with *syn* alignment have a smaller stabilization energy than the dimers with *anti* alignment, the respective energy differences for Et_2, nPr_2 and nBu_2 are 0.8 kJ/mol, 1.4 kJ/mol and 2.2 kJ/mol. *Anti* structures of small dimers, like Et_2, are more stable because the reduction of the destabilizing dispersionless interaction (2.2 kJ/mol) is stronger than the reduction of the attractive dispersion interaction (1.3 kJ/mol); in large dimers, like Bu_2, the dispersionless interaction is reduced by 0.8 kJ/mol but the attractive dispersion interaction enlarged by 1.4 kJ/mol (Table 8.5). The percentage of the dispersion energy in Me_2 is already 99% and increases to 137% in Bu_2.

By internal rotation in the alkyl groups with respect to C-C single bonds it is possible to create substituents with *clinal* conformations. For the Bu_2 dimer, we created start geometries for such structures by internal rotations in one substituent, the second was kept in the all-antiperiplanar conformation. Rotation of the propyl group by 90 degrees about the C_α-C_β bond yields the *cis-ab* conformer, rotation of the ethyl group by 90 degrees about the C_β-C_γ bond yields the *cis-bc* conformer. The optimized geometries are shown in Figure 8.13; the stabilization energies are -25.5 kJ/mol and -22.7 kJ/mol, respectively.

Small *gauche* dimers like Et_2 are more stable than the corresponding *cis* dimers, but for the larger substituents the trend changes and the *cis* isomers are more stable. For these dimers, the high flexibility of the alkyl chains allows that the terminal parts of the substituents come in close contact without strong stretching of the central moiety. This is not possible with small substituents, for example ethyl groups.

The four optimized *cis* and the *gauche* structures have stabilization energies

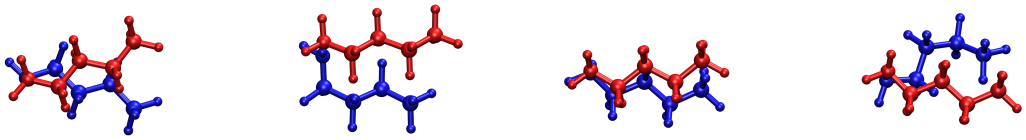

Figure 8.13: *cis* dimers of Bu_2. From left to right: *cis-anti*, *cis-ab*, *cis-syn*, *cis-bc*.

lying in an energy interval of 2.8 kJ/mol. If we make rotations about single bonds not only in one but in both substituents, we expect some more dimer structure having similar energies. With increasing length of the substituents the number of different equilibrium structures with similar stabilization energies will strongly increase.

Also for dimers with branched substituents we get structures with similar energies. Both stable structures for the iPr_2 and tBu_2 dimers have energies that differ by 2.1 kJ/mol. Although both repulsive dispersionless interaction energy and attractive dispersion energy are larger in the more stable dimers, it is the much larger attractive component, which is responsible for the strong stabilization.

That the balance of attractive dispersion interaction and repulsive dispersionless interaction is responsible for the dimer structures can be demonstrated by analyzing *zigzag* structures, which were found only with dlDF+D_{as}. See Table A.8 in Appendix. In *zigzag*-Me_2, each methyl group is not only near to the nitrogen atom it is bonded to, it is also much closer to the other nitrogen atom than it is in *trans*-Me_2. Due to a strong increase of exchange repulsion the dispersionless energy increases by 2.3 kJ/mol, making the dispersionless energy positive, thus destabilizing. However, also the attractive dispersion interaction is by 3.1 kJ/mol larger than in *trans*-Me_2, so that the sum of both contributions makes *zigzag*-Me_2 by 0.8 kJ/mol more stable than *trans*-Me_2. In *zigzag*-Et_2 the terminal methyl groups are still rather close to the central moiety, causing both an increase of dispersion interaction and dispersionless interaction and, concomitantly making *zigzag*-Et_2 by 1.2 kJ/mol

more stable than *zigzag*-Me_2; *zigzag*-Pr_2 dimer is by 1.1 kJ/mol more stable than *zigzag*-Et_2 and *zigzag*-Bu_2 is by 0.4 kJ/mol more stable than *zigzag*-Pr_2. We expect that convergence is reached for dimers with pentyl or hexyl substituents.

8.4.4 Origin of dimer stabilization

The stabilization energies converge in the *trans* series to the value for Pr_2, but in the *cis* and the *gauche* series the stabilization energies seem to grow constantly by a finite increment, which is about 3 kJ/mol per CH_2 group for *cis* dimers with *syn* alignment, about 4 kJ/mol per CH_2 group for *cis* dimers with *anti* alignment, and 1.5 kJ/mol per CH_2 group for *gauche* dimers. These constant increases of the stabilization energies are always due to a large increase in the stabilizing dispersion interaction and a smaller increase in the destabilizing dispersionless interaction. The latter is itself the sum of a large increment in the destabilizing exchange repulsion and a smaller increment in attractive electrostatics and induction. Although the individual interactions have different range, their sum is nevertheless short-ranged, and therefore each additional methylene group sees only the nearest atoms in the opposite alkyl chain. In the study of non-covalent interaction between carbon nanotubes and aromatic adsorbates we called the set of all intermolecular atom-pairs "seeing each other" the "contact zone" of the non-covalent interaction[73, 74, 75] and we showed that only atoms in the contact zone contribute to the interaction energy. The size of the contact zone is proportional to the intersection of the contact surfaces of the interacting molecules, as defined by Richards.[76] The intersection of contact surfaces is especially helpful for explaining the strong interaction between several parallel aligned alkyl chains and the much smaller interaction between globular alkyl groups, but it is not so helpful for analyzing the difference in interaction between *cis* and *trans* dimers. For doing this, we calculated the interaction energy of the intermolecular atom pairs lying inside a sphere with the midpoint in the

Table 8.5: Total interaction energy E_{Int}, dispersionless interaction energy E_{DL}, dispersion contribution E_{Das} of *trans* dimers at the equilibrium distances R_{Int}; the * indicates the interaction energies at the minima R_{DL} of the dispersionless energy E_{DL}. Energies in kJ/mol, distances in Å

System	R_{Int}	E_{Int}	E_{DL}	E_{Das}	R_{DL}	E^*_{DL}	E^*_{Int}
$(NH_3)_2$	3.30	-12.2	-5.0	-7.2	3.62	-6.8	-10.8
trans-Me_2	3.19	-15.4	-1.1	-14.3	3.66	-5.5	-11.9
trans-Et_2	3.19	-15.9	-0.7	-15.3	3.68	-5.4	-12.0
trans-nPr_2	3.18	-16.2	-0.6	-15.7	3.67	-5.4	-12.3
trans-nBu_2	3.18	-16.3	-0.5	-15.8	3.67	-5.4	-12.3
cis-Me_2	3.20	-16.8	-0.1	-16.7	3.69	-5.3	-12.5
cis-anti-Et_2	3.30	-18.2	2.3	-20.5	3.91	-4.5	-12.5
cis-anti-nPr_2	3.35	-21.9	6.4	-28.3	4.06	-3.7	-13.3
cis-anti-nBu_2	3.34	-25.5	9.5	-35.0	4.16	-3.4	-14.2
cis-syn-Et_2	3.25	-17.4	4.5	-21.8	3.92	-3.3	-11.1
cis-syn-nPr_2	3.28	-20.5	8.1	-28.6	4.07	-2.6	-11.4
cis-syn-nBu_2	3.36	-23.3	10.3	-33.6	4.23	-2.3	-11.7
gauche-Et_2	3.27	-19.1	5.2	-24.3	4.04	-3.6	-11.4
gauche-nPr_2	3.29	-21.7	7.3	-29.0	4.15	-3.3	-12.7
gauche-nBu_2	3.29	-23.0	8.2	-31.3	4.12	-3.1	-13.3
iPr_2I	3.19	-17.9	2.3	-20.2	3.78	-4.4	-12.5
iPr_2II	3.20	-20.0	4.1	-24.0	3.89	-4.2	-12.8
tBu_2I	3.25	-20.0	5.3	-25.3	3.99	-3.7	-13.0
tBu_2II	3.30	-17.9	3.3	-21.2	3.96	-3.8	-12.0

center of the central moiety and studied the increase in the interaction by gradually increasing the radius of the sphere, R_S. This method was also used in our study of the dispersion interaction between the substituents in alcohol dimers.[66] In Figure 8.14, we show the dispersion interaction E_{Das} for different dimers as a function of the increase ΔR_S of R_S, the zero of ΔR_S corresponds to R_S being half of the respective N$\cdots$N equilibrium distances, that is, half of the R_{Int} values from Table 8.5. In the ammonia dimer, the major contribution comes from the atoms of the N–H$\cdots$N central moiety, with increasing R_S the sphere contains the remaining five hydrogen atoms; increasing the radius by $\Delta R_S \approx 0.35$ Å, one additional hydrogen atom is inside the sphere, when R_S is approximately 2.5 Å, corresponding to $\Delta R_S \approx 0.9$ Å, also the remaining four hydrogen atoms lie inside the sphere. The first contributions to the interaction energy for *trans*-Me_2 come again from the atom pairs of the central moiety lying within the sphere with $R_S = 1.6$ Å, increase of R_S by $\Delta R_S \approx 0.4$ Å includes the carbon atoms of the methyl groups and therefore gives a large contribution to the interaction energy, all contributing intermolecular atom pairs lie within a sphere with $R_S = 2.5$ Å(or $\Delta R_S = 0.9$ Å) and further enlargement of R_S does not change E_{Das} anymore. The E_{Das} curve for *trans*-Et_2 looks very similar to the Me_2 curve, which means that only the α-CH_2 groups make substantial contributions to the interaction energy; this assumption is corroborated by the shape of the Pr_2 and Bu_2 curves, which are essentially identical to the Et_2 curve, as well as by the left subfigure of Figure 8.15, showing that CH_2 groups that are more distant than the diameter of the second sphere do not contribute to the stabilization.

The curves for the *cis* dimers look very different. The Me_2 curve becomes constant for $\Delta R_S \approx 0.9 Å$, as in the *trans* series, the magnitude of E_{Das} is slightly larger, because in the *cis* dimer the methyl groups not only see the atoms of the central moiety but also each other. When going from Me_2 to Et_2, the distance of the

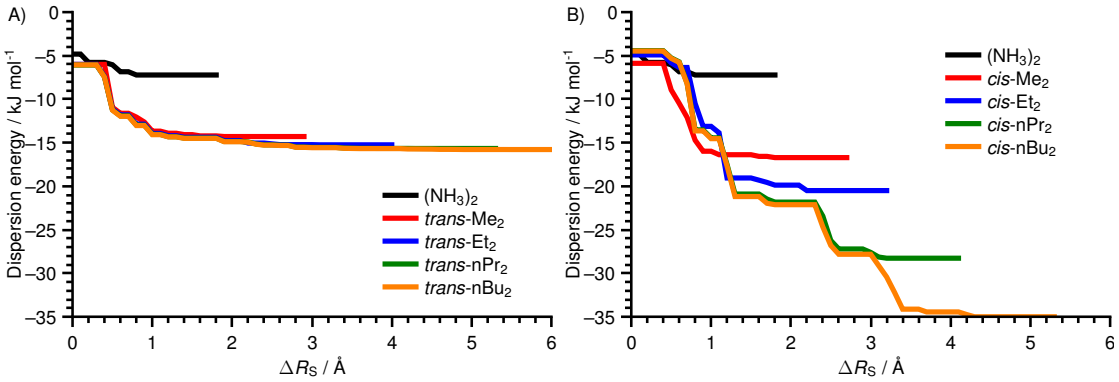

Figure 8.14: The cumulative increase of the dispersion contribution to dimer stability as a function of the increase ΔR_s; A) is the *trans*, and B) is the *cis-anti* series

terminal methyl group increases as in the *trans* series but now each methyl group not only "sees" the other methyl group, but also the neighboring CH_2 group. The Bu_2 curve shows nicely how the three CH_2 and the terminal CH_3 group contribute to E_{Das}: the first contribution from the substituents stems from the α CH_2 groups, which see the atoms of the central moiety as well as each other. The contributions of the β, γ, etc. groups are smaller than these of the α groups because each new CH_2 group sees only the opposite methyl and the neighboring CH_2 group but not the electron-rich atoms of the central moiety, however, these contributions are rather constant.

The equilibrium structures of *gauche* dimers with small substituents are different from both the *trans* and *cis* dimers; when the substituents increase the parts of the alkyl groups next to the central moiety are more distant than in a *cis* dimer but the more distant parts will adopt a parallel structure as in the *cis* series. In *gauche* Bu_2, the first contributions are smaller than in the *cis* dimer but the more distant parts of the butyl groups give similar contributions as for the *cis* dimer.

For branched, bulky substituents the development of the E_{Das} curves is in between the corresponding *trans* and *cis* curves (Figure 8.16. Amine dimers with bulky

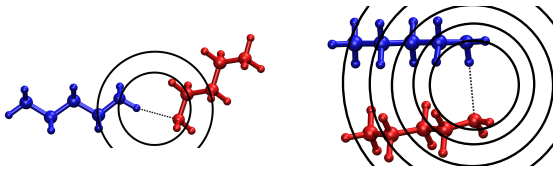

Figure 8.15: Spheres enclosing parts of nBu_2, the centers are the midpoint of the N-N distance, the radii R_s correspond to the positions of the jumps in the energy curve in Figure 8.14. Left for the *trans*, and right for the *cis* dimer.

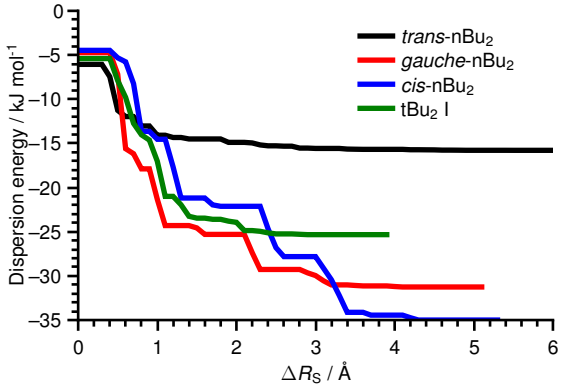

Figure 8.16: The cumulative increase of the dispersion contribution to the stability of four Bu_2 dimers as a function of ΔR_s.

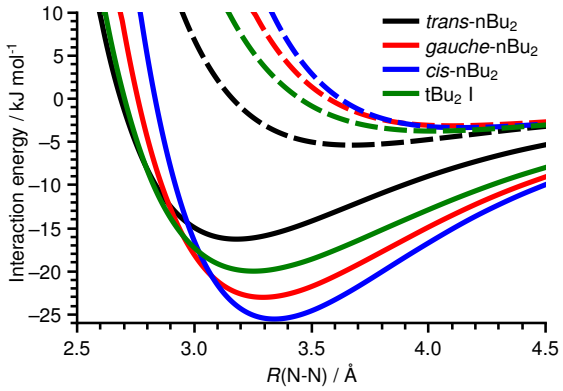

Figure 8.17: Total interaction energies (full lines) and dispersionless interaction energy (dashed lines) of different Bu isomers.

substituents are always *trans*-like, which means the bulky substituents are as far away from each other as possible. The growth of tBu_2 in the spherical shells shows first the contribution of the two α carbon atoms, which is smaller than that of two CH_2 groups in *trans*-Bu_2, and then the contributions of six methyl groups. Their contribution is larger than that of the two β-CH_2 groups, but smaller than the contribution of the four β and γ-CH_2 groups in *cis*-Bu_2. The different dispersion contributions determine the ordering of both the dispersionless and the total interaction energy curves, as shown in Figure 8.17 for the Bu_2 dimers.

8.5 Discussion

Our study does not support the assumption that amine dimers are solely stabilized by hydrogen bonds. The structure of the central moiety does not dramatically change when going from the eclipsed ammonia dimer to the amine dimers, but the stabilization energy increases considerably and, moreover, also depends on the size and position of the alkyl groups. This is incomprehensible if one believes that the atoms of the central moiety are responsible for hydrogen bonding. If one believes

that dispersion is less important than electrostatics for hydrogen bonding, it is hard to explain why the dispersionless stabilization energy is only a fraction of the total stabilization energy, and why the local minima of the dispersionless interaction energy are at much larger distances than the minima of the total interaction energy, and why correct stabilization energies are only obtained when dispersion interaction is accounted for.

Figure 8.18 shows the energy contributions to the dispersionless interaction energy for the water dimer as obtained from a SAPT study[66] of our working group together with the dispersionless interaction energy of the ammonia dimer, calculated with dlDF. Both dispersionless interaction energy curves have extremely shallow potential wells and a zero at about 85% of the positions of the respective minima. As the curves for the water dimer show, the dispersionless interaction energy at large distances is dominated by electrostatics and induction because exchange has already died away there; at short distances exchange dominates the dispersionless interaction energy. The slope at zero is the sum of the large positive slope of the attractive interaction and of the large negative slope of the repulsive exchange, it is, in magnitude, much smaller than either of the contributions. As the depths of the potential wells show, the contribution of electrostatics and induction in the ammonia dimer is much smaller than in the water dimer; the smaller slope for the ammonia dimer suggests that also the repulsive exchange is smaller in the ammonia dimer. Adding the dispersion contribution to the dispersionless interaction energy roughly doubles the well depths for both dimers, but as also the dispersion contribution for the ammonia dimer is smaller in magnitude, the stabilization energy for the ammonia dimer is still about half the stabilization energy for the water dimer. (Figure 8.19.) Adding the dispersion interaction shifts the minima of the total interaction energies to distances that are about 10% smaller than the minima of the dispersionless interaction energy curves, and also the zeros of the

total interaction energies are shifted to smaller distances. Without consideration of dispersion interactions, both dimers are more floppy and more unstable.

The qualitative agreement of the interaction energy curves for both dimers is striking and shows that 1) the assumption that the dominating attractive interaction is electrostatics is not true, dispersion interaction is at least as important and 2) representing exchange repulsion in a hydrogen bonded complex by a hard sphere potential is completely at odds with both the shapes of dispersionless and total interaction energies. Since dispersion depends on the polarizability of the interacting molecules and the polarizabilities of water and ammonia are determined by the heavy element atoms, that is, oxygen and nitrogen, we assume that these findings hold also for amine dimers and alcohol dimers. For dimers with atoms from periods higher than 2 this has to be proven.

Dispersion interaction is crucial for the molecular structure of non-polar molecules. Non-branched alkane molecules with up to 17 or 18 carbon atoms prefer an extended structure with the all-antiperiplanar conformation being most stable; larger molecules can adopt a hairpin structure but need at least four *gauche* dihedral angles to bring linear chain segments into contact.[77] The costs for these rotations are outweighed by the energy gain due to the interaction between the chain segments. In amine dimers, but also in alcohol dimers, the central moiety allows the hairpin structure in *cis* dimers without any additional costs for internal rotations, the *trans* conformer is not the most stable but the least stable conformer.

Condensed matter properties, like the boiling point, represent the strength of intermolecular interaction in the condensed phase. For water and ammonia, the boiling points are very different with +100 °C and -33 °C, respectively, for methanol and methylamine the difference between the boiling points of +65 °C and -6 °C, respectively, is already smaller, but for the n-decyl-substituted species they are already very similar, +231 °C and +221 °C, respectively. In both series, alcohols

and amines, we observe a monotonic increase of the boiling point with increasing length of the alkyl groups,[63] which demonstrates the increasing importance of the interaction between the substituents. After all, the atomic percent of the alkyl groups in butylamine is already 81%.

Comparison of the boiling points of all butyl-amines and butyl-alcohols shows the influence of the shape of the substituents: the boiling points for *n*-butylamine, *iso*-butylamine, *sec*-butylamine and *tert*-butylamine are 79 °C, 66 °C, 63 °C and 45 °C, respectively; the boiling points for the corresponding butyl alcohols are 118 °C, 108 °C, 99 °C and 83 °C, respectively.[78] In both series, the species with the linear *n*-butyl substituents have the highest and the species with the globular *tert*-butyl substituents have the lowest boiling points. The contact surfaces of *n*-alkyl chains can be regarded as tubes, whereas these of globular alkyl groups are roughly spheres. Accordingly, the contact zone for parallel aligned tubes is always much larger than that for spheres in close contact, the stronger interaction between the *n*-alkyl groups explains the higher values of the boiling points.

Stressing the role of dispersion interaction between large substituents does not mean that the polar groups forming the central moiety are unimportant; this would be completely wrong as, for example, the increase of the respective boiling points with increasing number of amino groups shows: the respective values for propylamine, 1,3-propanediamine and 1,2,3-propanetriamine are 49 °C[78], 139 °C[78] and 190 °C[79]. But the boiling points of 116 °C, 139 °C, 158 °C, 179 °C, and 204 °C for the series 1,2-diaminoethane, propane-1,3-diamine, butane-1,4-diamine, pentane-1,5-diamine and hexane-1,6-diamine,[78] show again that the boiling point also increases when the non-polar part of the molecule increases. The result of our investigations of the interactions between the substituents in dimers can be used to explain the interactions between dimers as well; the interaction between linear alkyl groups is the same irrespective of whether they belong to a single dimer or

to different dimers. The short range attractive interactions become operative as soon as the two alkyl chains are brought into close contact. In amines or alcohols, this is done by the central moiety; terminal polar groups in diamines or dioles will further reduce the distance between the alkyl chains and, thus, increase the attractive interaction between the substituents. The boiling point of 1-propanol with 4 heavy atoms and one polar OH group (97 °C[78]) is nearly identical with the 98 °C of heptane[78] having seven heavy atoms but no polar group. This means, there are strong attractive interactions between long alkyl chains even without polar groups forming hydrogen bonds, but hydrogen bridges enhance the attraction considerably. An analogy of the attraction between alkyl chains that are connected by hydrogen bonds is reinforced concrete: ubiquitous dispersion is the concrete and the hydrogen bridges are the rebars. Claiming that the bonding between polyalcohols or polyamines is only due to the hydrogen bridges, means ignoring the concrete and considering only the rebars. Stressing only the role of dispersion interaction would mean ignoring the rebars and considering only the concrete.

Internal rotation in long alkyl chains gives rise to a large number of rotamers; when several of them are parallel aligned this gives rise to a large number of equilibrium structures with similar stabilization energies. The high energetic degeneracy of such structures, which are absent in the gas phase, are the origin of the entropy term in the free energy that is necessary to understand hydrophobic interactions. The statement by Wolfenden and Lewis[14] "that a strong favorable interaction among alkane molecules in liquid alkanes gives a strong favorable transfer energy for passage of an alkane from vapor into liquid alkane" does not do justice to this phenomenon because it emphasizes only the energy contribution to the transfer free energy. The conformational entropy contribution must not be ignored.

If the atomic group connecting the substituents in a *cis* dimer is replaced by

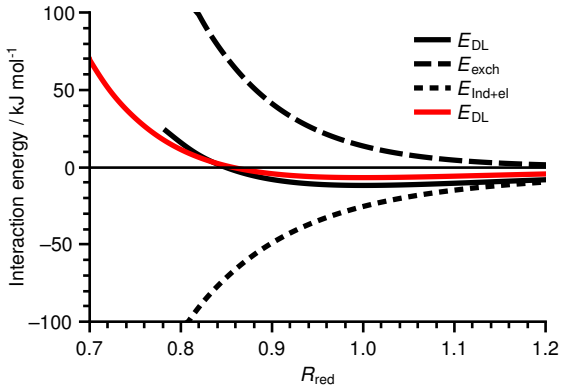

Figure 8.18: Black curves: SAPT energies (dispersionless, exchange and induction+exchange) of the water dimer. Red curve: dlDF energy of the ammonia dimer. The abscissa is the reduced inter-monomer distance $R_{\mathrm{red}} = R/R_{\mathrm{min}}$ at the minimum of the dispersionless energy curve.

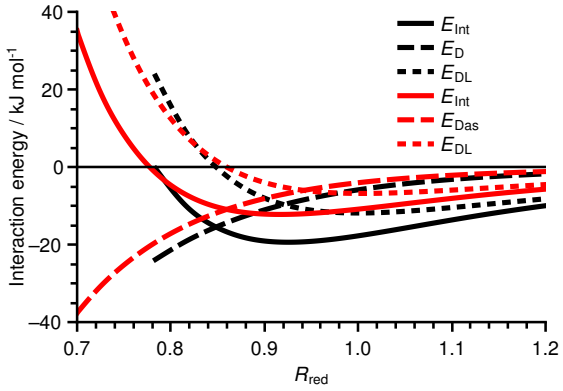

Figure 8.19: Total interaction, dispersion and dispersionless energies. Black curves: SAPT energies of the water dimer. Red curves: dlDF+D_{as} energies of the ammonia dimer. The abscissa is the reduced inter-monomer distance $R_{\mathrm{red}} = R/R_{\mathrm{min}}$ at the minimum of the dispersionless energy curve.

say an ether oxygen no one would say that the stability of the hairpin structure is caused by covalent bonding between the substituents and the bridging oxygen atom. Indeed the stability of such structures has to be attributed to intramolecular dispersion interaction[19], which is crucial for the understanding of the geometry of large molecular systems, as mentioned by Wagner.[10]

9 Conclusion

The stability of complexes with an A–H$\cdots$B atom group is often attributed to electrostatic interaction between atoms and/or atom groups in this central group, although weak, intermolecular interactions are composed of three attractive and one repulsive basic interactions, which act between all atoms in the complex not just between those in the central group. The role of electrostatic as attractive interaction is often grossly overstated and the role of dispersion is underrated.

This was shown by analyzing the interaction in complexes of small molecules containing atoms from group 14 to 17 like water, methane or hydrogenfluorid and their analogues with the heavy atoms replaced by the corresponding second row atoms. Because of the much larger distance between these atoms, all interactions are strongly reduced, in some cases the interaction is significantly stronger in complexes without a hydrogen bridge. These examples show that it is wrong to attribute stabilization of a complex solely to a hydrogen bridge.

The study of amine dimers with alkyl substituents of variable length shows that system stabilization can be dominated by attractive interactions, especially the dispersion, between the substituents, which can be much larger than the contribution of the central group.

Although in some complexes the electrostatic interaction may be very large and crucial for their stabilization, dispersion interaction is ubiquitous and stabilizing, irrespective of the occurrence of a strong electrostatic and induction interaction.

This is especially true for complexes with molecules having no low multipole moments like methane, silane or ethene.

The discussion of several amine dimers with large alkyl substituents having high number of energetical close equilibrium structures, generated by rotations around the carbon-carbon bonds, is the origin of the entropic part of the hydrophobic interaction, which is used to explain properties in liquid alkanes.

Appendix

From a SAPT(DFT) calculation we obtain several first, second and higher order contributions. The interaction energy is decomposed in several parts. The first-order terms the electrostatic energy, E_{elst}, and the exchange energy, E_{exch}. The second-order terms contains all kind of different components, induction energy, E_{Ind}, dispersion energy, E_{D} and their exchange counterparts, $E_{\text{D}-\text{exch}}$ and $E_{\text{Ind}-\text{exch}}$. The higher induction terms, $\delta_{\text{Ind,HF}}$ are estimated from a HF supermolecule calculation, in our case the same basis set as for the other components is used. The grouped total interaction energy is the given by following equation; giving the introduced four (global) interaction components:

$$E_{\text{Int,SAPT(DFT)}} = \underbrace{E^{(1)}_{\text{elst}}}_{E_{\text{elst}}} + \underbrace{E^{(1)}_{\text{exch}}}_{E_{\text{exch}}} + \underbrace{E^{(2)}_{\text{Ind}} + E^{(2)}_{\text{Ind}-\text{exch}} + \delta_{\text{Ind,HF}}}_{E_{\text{Ind}}} + \underbrace{E^{(2)}_{\text{D}} + E^{(2)}_{\text{D}-\text{exch}}}_{E_{\text{D}}}$$

The underlying functional leads to a problematic point: all parts containing exchange components cannot be described very well and give at most approximations.[16] For SAPT(DFT) calculations a asymptotic correction (AC) for the exchange-correlation potential is needed to achieve the right shape and to get meaningful results. The problem is: not changing the already correct short range part, while changing the long range part; a smoothing function is needed, connecting both parts. Also the underlying potential for the long range part is important, which

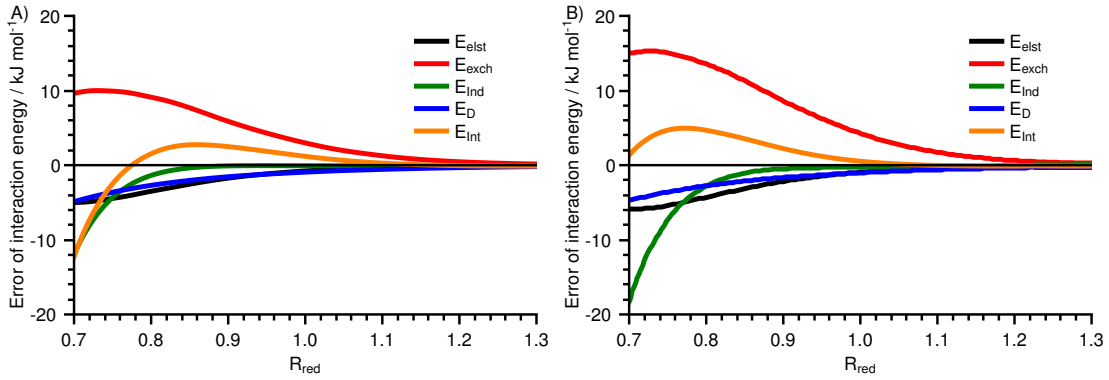

Figure A.1: Absolute errors of H_2S dimer (left) and HCl dimer (right) of the total interaction energy and the components.

differs in both presented versions. The SAPT(DFT) Delaware uses the Fermi-Amaldi potential, whereas the SAPT(DFT) MolPro2010 uses the Van Leeuwen and Baerends potential (for the AC part of the potential).[28]

In both version the asymptotic part is shifted by a constant value of the ionization potential IP and orbital energy of the highest occupied molecule orbital E_{HOMO}, so that the right asymptotic behavior is achieved. Typical a separate calculation with the respectively functional, for the cationic and neutral system, is done to extract these two parameters. The authors of the method in SAPT Delaware version recommended to use experimental IP.

As mentioned in the text the corresponding minimum of SAPT(DFT) is shifted by a relative distance of 0.05. To see whether Delaware version works better, we also calculated the potential curves in the same manner. The distance of the minimum is the same what we obtain with QCISD(T) after optimized the geometry (curves not shown here). The difference has to be in the single components; therefore we subtract MolPro2010 value from Delaware. The curves show that the main error at around $R_{\mathrm{red}} = 1$ is coming from the exchange component.

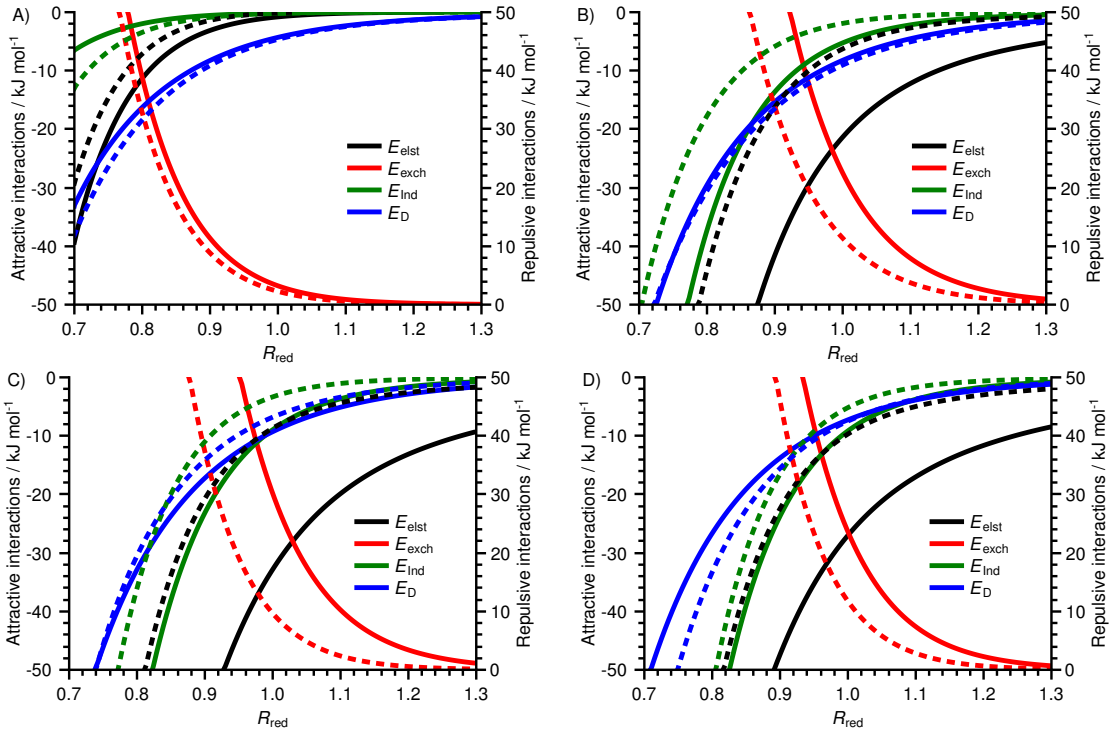

Figure A.2: Distance dependency of the single components electrostatic, induction, exchange and dispersion energy; the pairs (solid/dashed) A) $(CH_4)_2/(SiH_4)_2$, B) $(NH_3)_2/(PH_3)_2$, C) $(H_2O)_2/(H_2S)_2$ and D) $(HF)_2/(HCl)_2$

Table A.1: Total interaction energy and the basis set independent dispersion contribution of cyclic $(NH_3)_2$ (left) and *cis*-Me_2 (right) in kJ/mol

Basis	dlDF+D_{as}	B3LYP+D2	B3LYP+D3	dlDF+D_{as}	B3LYP+D2	B3LYP+D3
DZ	-11.12	-14.52	-12.26	-16.17	-19.32	-17.48
TZ	-12.76	-15.66	-13.40	-17.10	-19.72	-17.87
QZ	-12.69	-15.51	-13.26	-17.12	-19.74	-17.90
5Z	-12.57	-15.31	-13.06	-17.10	-19.73	-17.89
aDZ	-12.04	-14.88	-12.62	-16.79	-19.49	-17.65
aTZ	-12.55	-15.20	-12.95	-17.09	-19.68	-17.84
aQZ	-12.56	-15.26	-13.01	-17.15	-19.75	-17.90
a5Z	-12.51	-15.24	-12.99	-17.12	-19.75	-17.91
E_D	-9.27	-6.09	-3.84	-16.35	-10.73	-8.88

Table A.2: Total interaction energy and dispersion contribution of $(NH_3)_2$ with one hydrogen bond (left) and *trans*-Me_2 (right) with different basis sets in kJ/mol

Basis	dlDF+D_{as}	B3LYP+D2	B3LYP+D3	dlDF+D_{as}	B3LYP+D2	B3LYP+D3
DZ	-11.54	-13.62	-12.94	-14.66	-16.92	-15.53
TZ	-12.23	-13.55	-12.87	-15.43	-17.14	-15.75
QZ	-12.08	-13.39	-12.71	-15.40	-17.14	-15.75
5Z	-12.06	-13.36	-12.68	-15.38	-17.13	-15.74
aDZ	-11.63	-13.07	-12.39	-15.05	-16.84	-15.45
aTZ	-12.09	-13.30	-12.62	-15.42	-17.09	-15.70
aQZ	-12.08	-13.35	-12.67	-15.42	-17.14	-15.75
a5Z	-12.05	-13.36	-12.68	-15.41	-17.15	-15.76
E_D cor.	-6.99	-3.94	-3.26	-13.93	-8.52	-7.13

Table A.3: Total interaction energies in kJ/mol for cyclic $(NH_3)_2$ at supporting structures taken from BEGDB. DFT values are calculated with the aTZ basis, TZ values are given in brackets. CC means CCSD(T)/CBS.

$R(H\cdots N)_{rel}$	CC	dlDF+D_{as}	B3LYP+D2	B3LYP+D3
0.90	-10.08	-9.18 (-9.59)	-10.80 (-11.49)	-8.91 (-9.61)
0.95		-11.69 (-12.00)	-14.22 (-14.79)	-11.81 (-12.38)
1.00	-13.14	-12.55 (-12.76)	-15.20 (-15.66)	-12.95 (-13.40)
1.05		-12.40 (-12.53)	-14.53 (-14.87)	-12.97 (-13.31)
1.10		-11.71 (-11.78)	-13.12 (-13.37)	-12.27 (-12.51)
1.20	-9.87	-9.67 (-9.65)	-10.06 (-10.15)	-9.93 (-10.02)
1.50	-4.64	-4.52 (-4.42)	-4.26 (-4.21)	-4.46 (-4.41)
2.00	-1.51	-1.44 (-1.37)	-1.36 (-1.33)	-1.38 (-1.36)

Table A.4: Total interaction energies in kJ/mol for *cis*-Me_2 at supporting structures taken from BEGDB. DFT values are calculated with the aTZ basis, TZ values are given in brackets. CC means CCSD(T)/CBS.

$R(M_1\text{-}M_2)_{rel}$	CC	dlDF+D_{as}	B3LYP+D2	B3LYP+D3
0.90	-15.48	-15.15 (-15.14)	-18.95 (-18.89)	-15.49 (-15.44)
0.95	-17.11	-16.78 (-16.79)	-19.96 (-19.96)	-17.45 (-17.45)
1.00	-17.36	-17.09 (-17.10)	-19.68 (-19.72)	-17.84 (-17.87)
1.05	-16.78	-16.58 (-16.57)	-18.68 (-18.74)	-17.30 (-17.35)
1.10	-15.69	-15.58 (-15.57)	-17.19 (-17.26)	-16.24 (-16.31)
1.25	-11.67	-11.65 (-11.61)	-11.89 (-11.95)	-12.02 (-12.07)
1.50	-5.48	-5.43 (-5.33)	-5.04 (-5.01)	-5.36 (-5.33)
2.00	-1.63	-1.61 (-1.52)	-1.51 (-1.47)	-1.55 (-1.50)

Table A.5: Geometry parameters of *trans* dimers optimized with different DFT based methods (bond lengths in Å and bond angles in deg.)

	N-H	H$\cdots$N	N-N	NHN	$C_\alpha NNC_\alpha$	$C_\omega NNC_\omega$	C_ω-C_ω	CN^HN	N^HNC
$(NH_3)_2$									
dlDF+D_{as}	0.98	2.35	3.32	166					
B3LYP+D2	1.03	2.28	3.28	165					
B3LYP+D3	1.03	2.28	3.30	172					
trans-Me_2									
dlDF+D_{as}	0.98	2.25	3.21	164	-176		4.63	121	90
B3LYP+D2	1.03	2.21	3.17	155	-171		4.65	122	84
B3LYP+D3	1.03	2.22	3.22	163	-177		4.81	119	91
trans-Et_2									
dlDF+D_{as}	0.98	2.25	3.20	164	-175	-151	7.11	121	90
B3LYP+D3	1.03	2.23	3.21	161	-173	-148	7.34	121	90
trans-nPr_2									
dlDF+D_{as}	0.98	2.25	3.19	162	-172	-157	9.04	122	90
B3LYP+D3	1.03	2.22	3.20	159	-170	-154	9.46	122	89
trans-nBu_2									
dlDF+D_{as}	0.98	2.25	3.19	162	-172	-144	11.4	122	89
B3LYP+D3	1.03	2.23	3.21	159	-171	-142	11.92	122	88
iPr_2 I									
dlDF+D_{as}	0.98	2.25	3.20	164	-180			121	91
B3LYP+D3	1.03	2.22	3.21	162	-179			120	91
tBu_2 I									
dlDF+D_{as}	0.98	2.30	3.27	172	-135			113	106
B3LYP+D3	1.03	2.21	3.22	168	-132			113	101

Table A.6: Geometry parameters of *zigzag* and *gauche* dimers optimized with different DFT based methods (bond lengths in Å and bond angles in deg.)

	N-H	H···N	N-N	NHN	$C_\alpha NNC_\alpha$	$C_\omega NNC_\omega$	C_ω-C_ω	CN^HN	N^HNC
zigazg-Me_2									
dlDF+D_{as}	0.98	2.33	3.20	148	88		3.82	90	97
Me_2[1]									
B3LYP+D3	1.03	2.22	3.21	160	-60		3.84	106	88
dlDF+D_{as}	0.98	2.25	3.19	162	-62		3.77	106	88
zigzag-Et_2									
dlDF+D_{as}	0.98	2.37	3.22	145	96	166	5.46	92	91
gauche-Et_2									
B3LYP+D3	1.03	2.26	3.27	166	32	98	4.67	99	98
dlDF+D_{as}	0.98	2.34	3.28	162	35	101	4.56	100	97
zigzag-nPr_2									
dlDF+D_{as}	0.98	2.38	3.23	144	95	140	7.34	91	90
gauche-nPr_2									
B3LYP+D3	1.03	2.27	3.28	166	27	70	5.37	99	97
dlDF+D_{as}	0.98	2.35	3.29	161	29	71	5.21	99	96
zigzag-nBu_2									
dlDF+D_{as}	0.98	2.37	3.23	145	94	165	9.61	92	90
gauche-nBu_2									
B3LYP+D3	1.03	2.28	3.28	165	26	92	7.49	99	97
dlDF+D_{as}	0.98	2.36	3.30	161	29	95	7.22	99	96

[1]This structure is very similar to *cis*-Me_2 and differs only in the helicity.

Table A.7: Geometry parameters of *cis-syn* and *cis-anti* dimers as well as branched dimers optimized with different DFT based methods (bond lengths in Å and bond angles in deg.)

	N-H	H···N	N-N	NHN	$C_\alpha NNC_\alpha$	$C_\omega NNC_\omega$	C_ω-C_ω	CN^HN	N^HNC
cis-Me_2									
dlDF+D_{as}	0.98	2.26	3.20	161	71		3.81	104	88
B3LYP+D3	1.03	2.22	3.21	162	72		3.89	103	88
syn-Et_2									
dlDF+D_{as}	0.98	2.34	3.26	158	-50	-50	4.14	110	94
B3LYP+D3	1.03	2.26	3.28	169	-40	-42	4.17	110	106
anti-Et_2									
dlDF+D_{as}	0.98	2.33	3.31	176	-15	49	4.01	111	108
B3LYP+D3	1.03	2.25	3.28	179	-24	42	4.17	110	109
syn-nPr_2									
dlDF+D_{as}	0.98	2.39	3.28	151	-37	-38	4.60	107	90
B3LYP+D3	1.03	2.31	3.29	158	-37	-37	4.68	105	94
anti-nPr_2									
dlDF+D_{as}	0.98	2.37	3.35	172	-26	15	4.17	108	104
B3LYP+D3	1.03	2.27	3.31	178	-32	11	4.23	108	104
syn-nBu_2									
dlDF+D_{as}	0.98	2.46	3.36	152	13	14	4.26	101	97
B3LYP+D3	1.03	2.36	3.34	159	19	18	4.21	100	99
anti-nBu_2									
dlDF+D_{as}	0.98	2.37	3.35	173	-31	35	4.45	108	104
B3LYP+D3	1.03	2.28	3.31	178	-34	33	4.48	108	104
iPr_2 II									
dlDF+D_{as}	0.98	2.25	3.21	166	-109			112	93
B3LYP+D3	1.03	2.22	3.23	167	-89			113	99
tBu_2 II									
dlDF+D_{as}	0.98	2.35	3.31	166	80			121	117
B3LYP+D3	1.03	2.28	3.29	167	61			118	117

Table A.8: cc-pVTZ energies of the dimers calculated with two types of functionals with dispersion (correction) in kJ/mol. All geometries were optimized with dlDF+D_{as} and cc-pVDZ, B3LYP+D3 energies were calculated on structures that were reoptimized with B3LYP+D3.

	N-N	E_{Int}	E_{DL}	E_{Das}	N-N	E_{Int}	E_{B3LYP}	E_{D3}
$(NH_3)_2$	3.32	-12.23	-5.24	-6.99	3.30	-13.48	-10.34	-3.14
trans-Me_2	3.21	-15.43	-1.49	-13.93	3.22	-16.72	-10.14	-6.58
trans-Et_2	3.20	-15.89	-0.92	-14.98	3.21	-16.90	-9.76	-7.14
trans-nPr_2	3.19	-16.23	-0.89	-15.34	3.20	-17.16	-9.64	-7.53
trans-nBu_2	3.19	-16.27	-0.77	-15.49	3.21	-17.18	-9.55	-7.63
iPr_2 I	3.20	-17.90	1.78	-19.67	3.21	-18.70	-8.18	-10.52
tBu_2 I	3.27	-19.97	4.63	-24.60	3.22	-23.47	-6.35	-17.11
zigazg-Me_2	3.20	-16.18	0.84	-17.02				
gauche-Me_2	3.19	-16.90	-0.13	-16.77	3.21	-17.90	-9.39	-8.51
zigzag-Et_2	3.22	-17.57	4.66	-22.23				
gauche-Et_2	3.28	-19.09	4.82	-23.90	3.27	-20.51	-5.54	-14.97
zigzag-nPr_2	3.23	-18.67	5.66	-24.33				
gauche-nPr_2	3.29	-21.69	7.25	-28.94	3.28	-22.90	-4.55	-18.35
zigzag-nBu_2	3.23	-19.08	6.09	-25.18				
gauche-nBu_2	3.30	-23.02	7.77	-30.79	3.28	-24.09	-3.97	-20.12
cis-Me_2	3.20	-16.81	-0.09	-16.72	3.21	-17.65	-9.27	-8.38
syn-Et_2	3.26	-17.36	4.04	-21.40	3.28	-18.59	-6.65	-11.93
anti-Et_2	3.31	-18.19	2.11	-20.30	3.28	-20.26	-7.20	-13.05
syn-nPr_2	3.28	-20.54	8.05	-28.59	3.29	-21.65	-3.56	-18.09
anti-nPr_2	3.35	-21.86	6.45	-28.31	3.31	-23.87	-5.29	-18.58
syn-nBu_2	3.36	-23.34	10.29	-33.63	3.34	-25.22	-1.16	-24.06
anti-nBu_2	3.35	-25.54	9.28	-34.82	3.31	-27.63	-3.65	-23.98
iPr_2 II	3.21	-19.95	3.66	-23.61	3.23	-22.00	-8.43	-13.57
tBu_2 II	3.31	-17.86	2.95	-20.81	2.29	-20.60	-4.56	-16.05

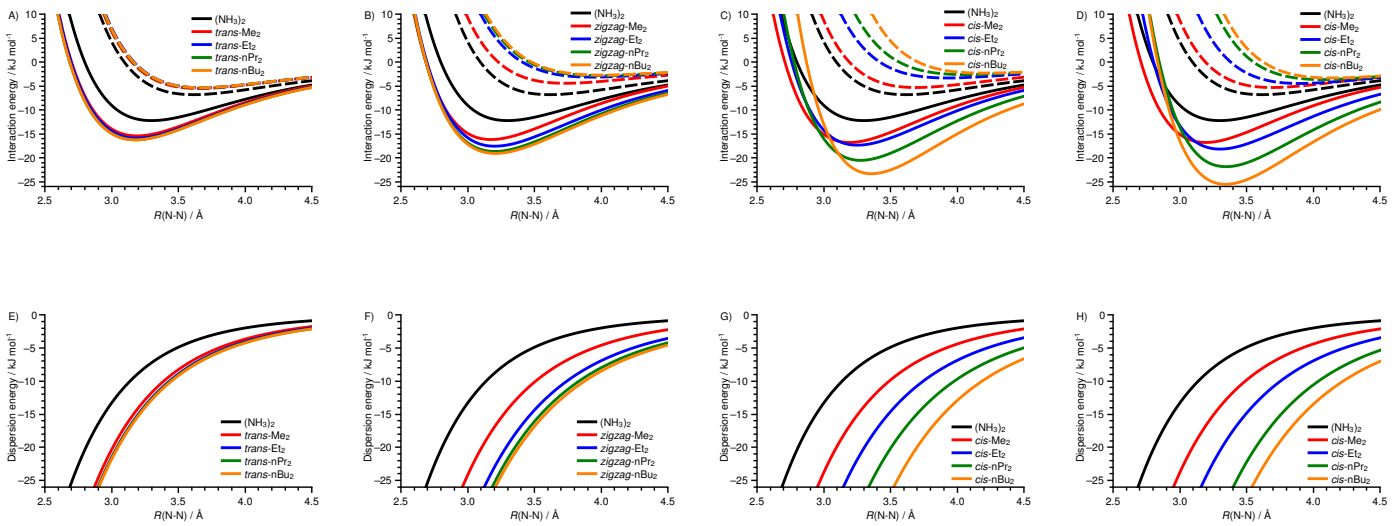

Figure A.3: Different interaction energy curves (A - D) showing total interaction energy (full lines) and dispersionless interction energy (dashed lines); and dispersion curves (E - H); starting from left to right with increasing stability *trans*, *zigzag*, *cis-syn* and *cis-anti*.

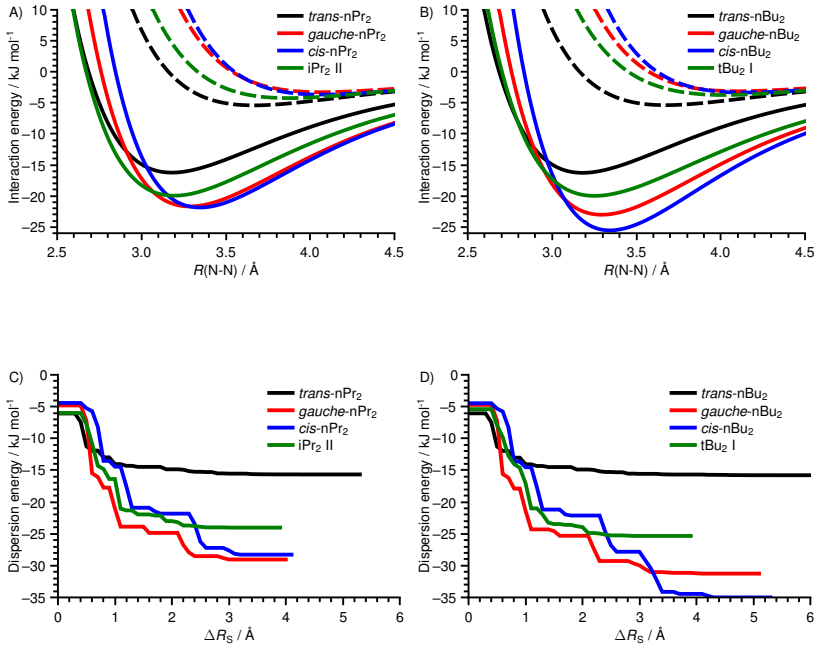

Figure A.4: Different interaction energy curves (A - B) showing total interaction energy (full lines) and dispersionless interction energy (dashed lines); and cumulative dispersion curves (C - D) of the different Pr_2 and Bu_2 dimers. The abscissa in C) and D) is the increase ΔR_S of the radius R_S starting from half of the respective N$\cdots$N equilibrium distances.

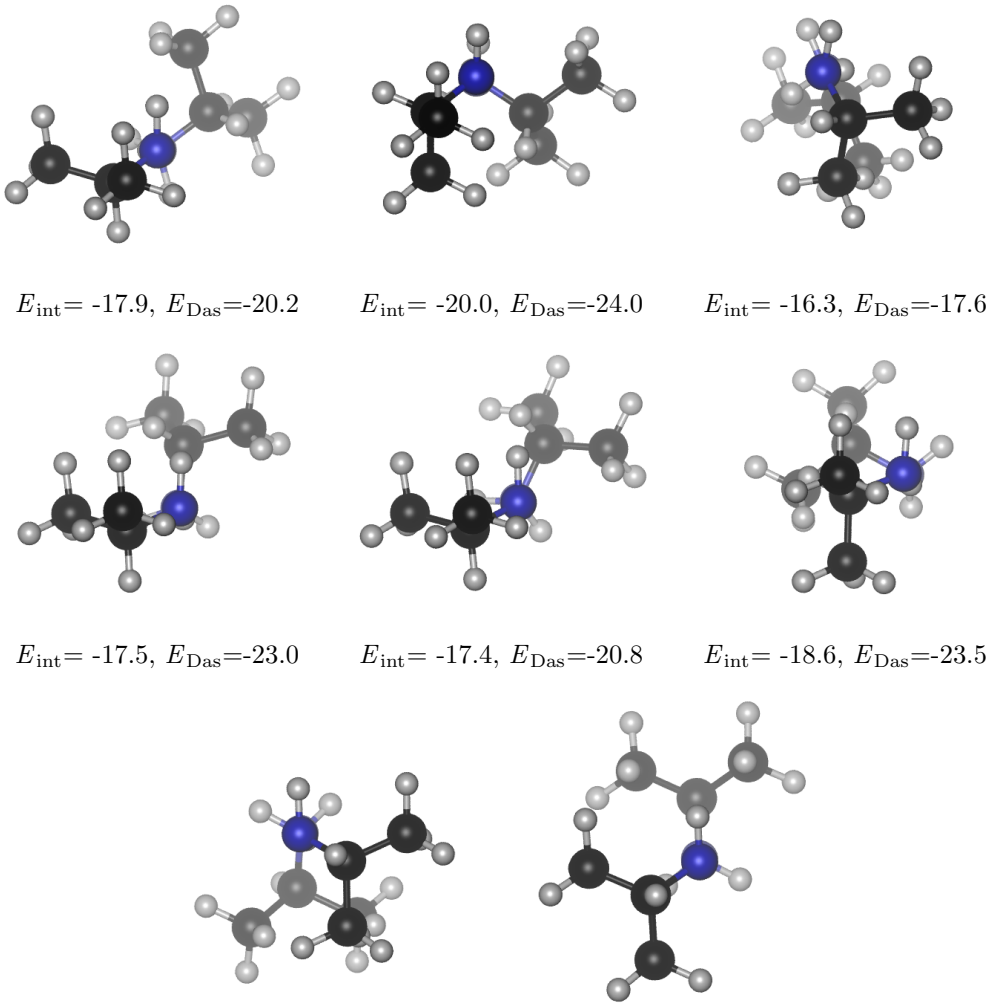

E_{int}= -17.9, E_{Das}=-20.2 E_{int}= -20.0, E_{Das}=-24.0 E_{int}= -16.3, E_{Das}=-17.6

E_{int}= -17.5, E_{Das}=-23.0 E_{int}= -17.4, E_{Das}=-20.8 E_{int}= -18.6, E_{Das}=-23.5

E_{int}= -16.2, E_{Das}=-19.2 E_{int}= -16.6, E_{Das}=-20.2

Figure A.5: Eight optimized iPr_2 structures with aligned nitrogen atoms. Interaction energies in kJ/mol; all N-N distances are between 3.2 and 3.3 Å.

List of Figures

List of Tables

List of Tables

Bibliography

[1] R. Rohs, S. West, A. Sosinsky, P. Liu, R. Mann, and B. Honig, "The role of dna shape in protein-dna recognition," *Nature*, vol. 461, no. 7268, pp. 1248–1253, **2009**.

[2] G. A. Jeffrey, *An Introduction to Hydrogen Bonding*. New York: Oxford University Press, **1997**.

[3] G. R. Desiraju and T. Steiner, *The Weak Hydrogen Bond*. New York: Oxford University Press, **2001**.

[4] A. Geim and I. Grigorieva, "Van der waals heterostructures," *Nature*, vol. 499, no. 7459, pp. 419–425, **2013**.

[5] K. T. Mahmudov, M. N. Kopylovich, M. F. C. G. da Silva, and A. J. Pombeiro, "Non-covalent interactions in the synthesis of coordination compounds: Recent advances," *Coordination Chemistry Reviews*, vol. 345, pp. 54 – 72, **2017**.

[6] M. Ahmad, W. Gu, T. Geyer, and V. Helms, "Adhesive water networks facilitate binding of protein interfaces," *Nat. Commun.*, vol. 2, no. 1, **2011**.

[7] J. Guo, X. Meng, J. Chen, J. Peng, J. Sheng, X.-Z. Li, L. Xu, J.-R. Shi, E. Wang, and Y. Jiang, "Real-space imaging of interfacial water with submolecular resolution," *Nat. Mater.*, vol. 13, no. 2, pp. 184–189, **2014**.

[8] S. J. Grabowski, *Hydrogen Bonding - New Insights*. Dortrecht: Springer, **2006**.

[9] G. Gilli and P. Gilli, *The Nature of the Hydrogen Bond*. New York: Oxford University Press, **2009**.

[10] J. P. Wagner and P. R. Schreiner, "London dispersion in molecular chemistry - reconsidering steric effects.," *Angewandte Chemie, International Edition*, vol. 54, pp. 12274–12296, **2015**.

[11] R. L. Baldwin, "The new view of hydrophobic free energy.," *FEBS Letters*, vol. 587, pp. 1062–1066, **2013**.

[12] W. Kauzmann, "Factors in interpretation of protein denaturation.," *Adv. Protein Chem.*, vol. 14, pp. 1–63, **1959**.

[13] R. L. Baldwin, *Weak Interactions in Protein Folding: Hydrophobic Free Energy, van der Waals Interactions, Peptide Hydrogen Bonds, and Peptide Solvation*. Weinheim: Wiley-VCH, **2014**.

[14] R. Wolfenden and C. A. Lewis Jr., "A vapor phase analysis of the hydrophobic effect.," *J. Theor. Biol.*, vol. 59, pp. 235–321, **1976**.

[15] I. G. Kaplan, *Intermolecular Interactions: Physical Picture, Computational Methods and Model Potentials*. John Wiley and Sons, **2006**.

[16] A. Stone, *The Theory of Intermolecular Forces, 2nd Edition*. Oxford University Press, **2013**.

[17] A. Salam, *Non-Relativistic QED Theory of the van der Waals Dispersion Interaction*. Springer, **2016**.

[18] S. Grimme, "Density functional theory with london dispersion corrections," *Wiley Interdisciplinary Reviews: Computational Molecular Science*, vol. 1, no. 2, pp. 211–228, **2011**.

[19] S. Grimme, A. Hansen, J. G. Brandenburg, and C. Bannwarth, "Dispersion-corrected mean-field electronic structure methods," *Chem. Rev.*, vol. 116, pp. 5105–5154, **2016**.

[20] C. Coulson, *Valence*. Clarendon Press, **1952**.

[21] F. Jensen, *Introduction to Computational Chemistry*. New York: John Wiley & Sons, 2 ed., **2006**.

[22] A. Szabo and N. S. Ostlund, *Modern Quantum Chemistry - Introduction to Advanced Electronic Structure Theory*. New York: Courier Corporation, revised ed. ed., **1996**.

[23] P.-O. Löwdin, "Quantum theory of many-particle systems. iii. extension of the hartree-fock scheme to include degenerate systems and correlation effects," *Phys. Rev.*, vol. 97, pp. 1509–1520, Mar **1955**.

[24] J. A. Pople, M. Head-Gordon, and K. Raghavachari, "Quadratic configuration interaction. A general technique for determining electron correlation energies," *The Journal of Chemical Physics*, vol. 87, no. 10, pp. 5968–5975, **1987**.

[25] C. Møller and M. S. Plesset, "Note on an Approximation Treatment for Many-Electron Systems," *Physical Review*, vol. 46, pp. 618–622, Oct. **1934**.

[26] B. Jeziorski, R. Moszyński, and K. Szalewicz, "Perturbation theory approach to intermolecular potential energy surfaces of van der Waals complexes," *Chem. Rev.*, vol. 94, pp. 1887–1930, **1994**.

[27] D. Tozer and N. Handy, "Improving virtual kohn-sham orbitals and eigenvalues: Application to excitation energies and static polarizabilities," *Journal of Chemical Physics*, vol. 109, no. 23, pp. 10180–10189, **1998**.

[28] M. Grüning, O. Gritsenko, S. Van Gisbergen, and E. Baerends, "Shape corrections to exchange-correlation potentials by gradient-regulated seamless connection of model potentials for inner and outer region," *Journal of Chemical Physics*, vol. 114, no. 2, pp. 652–660, **2001**.

[29] T. Dunning Jr., "Gaussian basis sets for use in correlated molecular calculations. i. the atoms boron through neon and hydrogen," *The Journal of Chemical Physics*, vol. 90, no. 2, pp. 1007–1023, **1989**.

[30] R. Kendall, T. Dunning Jr., and R. Harrison, "Electron affinities of the first-row atoms revisited. systematic basis sets and wave functions," *The Journal of Chemical Physics*, vol. 96, no. 9, pp. 6796–6806, **1992**.

[31] D. Woon and T. Dunning Jr., "Gaussian basis sets for use in correlated molecular calculations. iii. the atoms aluminum through argon," *The Journal of Chemical Physics*, vol. 98, no. 2, pp. 1358–1371, **1993**.

[32] D. Woon and T. Dunning Jr., "Gaussian basis sets for use in correlated molecular calculations. iv. calculation of static electrical response properties," *The Journal of Chemical Physics*, vol. 100, no. 4, pp. 2975–2988, **1994**.

[33] W. Klopper, R. Bachorz Rafa A., C. Hättig, and D. Tew, "Accurate computational thermochemistry from explicitly correlated coupled-cluster theory," *Theoretical Chemistry Accounts*, vol. 126, no. 5, pp. 289–304, **2010**.

[34] A. Halkier, T. Helgaker, P. Jørgensen, W. Klopper, H. Koch, J. Olsen, and A. Wilson, "Basis-set convergence in correlated calculations on ne, n_2 , and h_2o," *Chemical Physics Letters*, vol. 286, no. 3-4, pp. 243–252, **1998**.

[35] D. Schwenke, "The extrapolation of one-electron basis sets in electronic structure calculations: How it should work and how it can be made to work," *Journal of Chemical Physics*, vol. 122, no. 1, **2005**.

[36] S. Parthiban and J. Martin, "Assessment of w1 and w2 theories for the computational of electron affinities, ionization potentials, heats of formation, and proton affinities," *Journal of Chemical Physics*, vol. 114, no. 14, pp. 6014–6029, **2001**.

[37] J. Martin and G. De Oliveira, "Towards standard methods for benchmark quality ab initio thermochemistry - w1 and w2 theory," *Journal of Chemical Physics*, vol. 111, no. 5, pp. 1843–1856, **1999**.

[38] S. Boys and F. Bernardi, "The calculation of small molecular interactions by the differences of separate total energies. some procedures with reduced errors," *Molecular Physics*, vol. 19, no. 4, pp. 553–566, **1970**.

[39] L. Burns, M. Marshall, and C. Sherrill, "Comparing counterpoise-corrected, uncorrected, and averaged binding energies for benchmarking noncovalent interactions," *Journal of Chemical Theory and Computation*, vol. 10, no. 1, pp. 49–57, **2014**.

[40] H.-J. Werner, P. J. Knowles, G. Knizia, F. R. Manby, M. Schütz, P. Celani, T. Korona, R. Lindh, A. Mitrushenkov, G. Rauhut, K. R. Shamasundar, T. B. Adler, R. D. Amos, A. Bernhardsson, A. Berning, D. L. Cooper, M. J. O. Deegan, A. J. Dobbyn, F. Eckert, E. Goll, C. Hampel, A. Hesselmann, G. Hetzer, T. Hrenar, G. Jansen, C. Köppl, Y. Liu, A. W. Lloyd, R. A. Mata, A. J. May, S. J. McNicholas, W. Meyer, M. E. Mura, A. Nicklass, D. P. O'Neill, P. Palmieri, K. Pflüger, R. Pitzer, M. Reiher, T. Shiozaki, H. Stoll, A. J. Stone,

R. Tarroni, T. Thorsteinsson, M. Wang, and A. Wolf, "Molpro, version 2010, a package of ab initio programs," 2010. see http://www.molpro.net.

[41] A. Heßelmann, G. Jansen, and M. Schütz, "Density-functional theory-symmetry-adapted intermolecular perturbation theory with density fitting: A new efficient method to study intermolecular interaction energies," *Journal of Chemical Physics*, vol. 122, no. 1, **2005**.

[42] A. Heßelmann and G. Jansen, "First-order intermolecular interaction energies from Kohn-Sham orbitals," *Chemical Physics Letters*, vol. 357, no. 5-6, pp. 464–470, **2002**.

[43] TURBOMOLE V6.6 2014, a development of University of Karlsruhe and Forschungszentrum Karlsruhe GmbH, 1989-2007, TURBOMOLE GmbH, since 2007; available from `http://www.turbomole.com`.

[44] F. Weigend, A. Köhn, and C. Hättig, "Efficient use of the correlation consistent basis sets in resolution of the identity MP2 calculations," *The Journal of Chemical Physics*, vol. 116, no. 8, pp. 3175–3183, **2002**.

[45] C. Hättig, A. Hellweg, and A. Köhn, "Distributed memory parallel implementation of energies and gradients for second-order Møller-Plesset perturbation theory with the resolution-of-the-identity approximation," *Physical Chemistry Chemical Physics*, vol. 8, no. 10, pp. 1159–1169, **2006**.

[46] J. Řezáč, P. Jurečka, K. Riley, J. Černý, H. Valdes, K. Pluháčková, K. Berka, T. Řezáč, M. Pitoňák, J. Vondrášek, and P. Hobza, "Quantum chemical benchmark energy and geometry database for molecular clusters and complex molecular systems (www.begdb.com): A users manual and examples," vol. 73, no. 10, pp. 1261–1270, **2008**.

[47] M. D. Hanwell, D. E. Curtis, D. C. Lonie, T. Vandermeersch, E. Zurek, and G. R. Hutchison, "Avogadro: an advanced semantic chemical editor, visualization, and analysis platform," *Journal of Cheminformatics*, vol. 4, no. 1, p. 17, **2012**.

[48] A. D. Becke, "Density-Functional Thermochemistry. III. The Role of Exact Exchange," *J. Chem. Phys.*, vol. 98, no. 7, pp. 5648 – 5652, **1993**.

[49] S. Grimme, "Semiempirical gga-type density functional constructed with a long-range dispersion correction," *Journal of Computational Chemistry*, vol. 27, no. 15, pp. 1787–1799, **2006**.

[50] M. Sierka, C. Tuma, and T. Kerber 2011. Humboldt Universität, Berlin.

[51] A. D. Boese, M. Kirchner, G. A. Echeverria, and R. Boese, "Ethyl Acetate: X-ray, Solvent and Computed Structures," *ChemPhysChem*, vol. 14, no. 4, pp. 799–804, **2013**.

[52] A. Boese, "Basis set limit coupled-cluster studies of hydrogen-bonded systems," *Molecular Physics*, vol. 113, no. 13-14, pp. 1618–1629, **2015**.

[53] J. Řezáč and P. Hobza, "Extrapolation and scaling of the DFT-SAPT interaction energies toward the basis set limit," *Journal of Chemical Theory and Computation*, vol. 7, no. 3, pp. 685–689, **2011**.

[54] R. Bukowski, W. Cencek, P. Jankowski, M. Jeziorska, B. Jeziorski, S. A. Kucharski, V. F. Lotrich, M. P. Metz, A. J. Misquitta, R. Moszyński, K. Patkowski, R. Podeszwa, F. Rob, S. Rybak, K. Szalewicz, H. L. Williams, R. J. Wheatley, P. E. S. Wormer, and P. S. Żuchowski, "SAPT2016: An *ab initio* program for many-body symmetry-adapted perturbation theory calculations of intermolecular interaction energies." University of Delaware and University of Warsaw, **2016**.

[55] B. Jeziorski, R. Moszyński, and K. Szalewicz, "Perturbation theory approach to intermolecular potential energy surfaces of van der Waals complexes," *Chem. Rev.*, vol. 94, pp. 1887–1930, **1994**.

[56] A. Misquitta, R. Podeszwa, B. Jeziorski, and K. Szalewicz, "Intermolecular potentials based on symmetry-adapted perturbation theory with dispersion energies from time-dependent density-functional calculations," *Journal of Chemical Physics*, vol. 123, no. 21, **2005**.

[57] R. Podeszwa, R. Bukowski, and K. Szalewicz, "Density-fitting method in symmetry-adapted perturbation theory based on kohn-sham description of monomers," *Journal of Chemical Theory and Computation*, vol. 2, no. 2, pp. 400–412, **2006**.

[58] Dalton, a molecular electronic structure program, Release 2.0 (2005), see http://daltonprogram.org.

[59] M. Schmidt, K. Baldridge, J. Boatz, S. Elbert, M. Gordon, J. Jensen, S. Koseki, N. Matsunaga, K. Nguyen, S. Su, T. Windus, M. Dupuis, and J. Montgomery, J.A., "General atomic and molecular electronic structure system," *Journal of Computational Chemistry*, vol. 14, no. 11, pp. 1347–1363, **1993**.

[60] R. Weast, *CRC Handbook of Chemistry and Physics - A Ready-reference Book of Chemical and Physical Data*. CRC Press, 58 ed., **1977**.

[61] A. D. Boese, A. Chandra, J. M. L. Martin, and D. Marx, "From ab initio quantum chemistry to molecular dynamics: The delicate case of hydrogen bonding in ammonia," *The Journal of Chemical Physics*, vol. 119, pp. 5965–5980, Sept. **2003**.

[62] A. D. Boese, "Density functional theory and hydrogen bonds: Are we there yet?," *ChemPhysChem*, vol. 16, no. 5, pp. 978–985, **2015**.

[63] W. M. E. Haynes, *CRC Handbook of Chemistry and Physics, 94th Edition*. CRC Press, **2013**.

[64] A. J. Stone, "Are Halogen Bonded Structures Electrostatically Driven?," *Journal of the American Chemical Society*, vol. 135, no. 18, pp. 7005–7009, **2013**. PMID: 23581907.

[65] L. Gráfová, M. Pitoňák, J. Řezáč, and P. Hobza, "Comparative study of selected wave function and density functional methods for noncovalent interaction energy calculations using the extended s22 data set," *Journal of Chemical Theory and Computation*, vol. 6, no. 8, pp. 2365–2376, **2010**.

[66] J. Hoja, A. F. Sax, and K. Szalewicz, "Is electrostatics sufficient to describe hydrogen-bonding interactions?," *Chemistry - A European Journal*, vol. 20, no. 8, pp. 2292–2300, **2014**.

[67] K. Pernal, R. Podeszwa, K. Patkowski, and K. Szalewicz, "Dispersionless density functional theory," *Physical Review Letters*, vol. 103, no. 26, **2009**.

[68] A. Hesselmann, G. Jansen, and M. Schütz, "Density-functional theory-symmetry-adapted intermolecular perturbation theory with density fitting: A new efficient method to study intermolecular interaction energies," *J. Chem. Phys.*, vol. 122, p. 014103, **2005**.

[69] R. Podeszwa, K. Pernal, K. Patkowski, and K. Szalewicz, "Extension of the hartree-fock plus dispersion method by first-order correlation effects," *Journal of Physical Chemistry Letters*, vol. 1, no. 2, pp. 550–555, **2010**.

[70] S. Grimme, J. Antony, S. Ehrlich, and H. Krieg, "A consistent and accurate ab initio parametrization of density functional dispersion correction (dft-d) for the 94 elements h-pu," *Journal of Chemical Physics*, vol. 132, no. 15, **2010**.

[71] M. Valiev, E. Bylaska, N. Govind, K. Kowalski, T. Straatsma, H. V. Dam, D. Wang, J. Nieplocha, E. Apra, T. Windus, and W. de Jong, "Nwchem: A comprehensive and scalable open-source solution for large scale molecular simulations," *Computer Physics Communications*, vol. 181, no. 9, pp. 1477 – 1489, **2010**.

[72] J. Řezáč, K. E. Riley, and P. Hobza, "S66: A well-balanced database of benchmark interaction energies relevant to biomolecular structures," *Journal of Chemical Theory and Computation*, vol. 7, no. 8, pp. 2427–2438, **2011**.

[73] R. J. Maurer and A. F. Sax, "Solvation of carbon nanotubes by aniline calculated with density functional tight binding.," *Phys. Chem. Chem. Phys.*, vol. 12, pp. 9893–9899, **2010**.

[74] S. Glanzer and A. F. Sax, "Carbon Nanotubes Dressed by Aromatic Molecules," *Mol. Phys.*, vol. 111, no. 16-17, pp. 2427–2438, **2013**.

[75] C. Lechner and A. F. Sax, "Towards atomic-level mechanics: Adhesive forces between aromatic molecules and carbon nanotubes," **2017**. Applied Surface Science, doi=10.1016/j.apsusc.2017.05.170.

[76] F. M. Richards, "Areas, Volumes, Packing, and Protein Structure," *Annual Review of Biophysics and Bioengineering*, vol. 6, no. 1, pp. 151–176, **1977**.

[77] N. O. B. Luettschwager, T. N. Wassermann, R. A. Mata, and M. A. Suhm, "The last globally stable extended alkane.," *Angewandte Chemie, International Edition*, vol. 52, pp. 463–466, **2013**.

[78] GESTIS-Stoffdatenbank. Website, 2016. "http://www.dguv.de/ifa/gestis/gestis-stoffdatenbank/index.jsp",Online; accessed 21 November 2016.

[79] ChemSpider. Website, 2016. "http://www.chemspider.com/",Online; accessed 21 November 2016.